CONSTRAINING MECHANISTIC MODELS OF INDICATOR BACTERIA AT RECREATIONAL BEACHES IN LAKE MICHIGAN USING EASILY-MEASURABLE ENVIRONMENTAL VARIABLES

By

Aaron Wendzel

A THESIS

Submitted to
Michigan State University
in partial fulfillment of the requirements
for the degree of

Environmental Engineering—Master of Science

2014

ABSTRACT

CONSTRAINING MECHANISTIC MODELS OF INDICATOR BACTERIA AT RECREATIONAL BEACHES IN LAKE MICHIGAN USING EASILY-MEASURABLE ENVIRONMENTAL VARIABLES

By

Aaron Wendzel

Beach closures have significant economic and human health implications. The ability to create and use near-real time hydrodynamic and transport models that simulate fecal indicator bacteria (FIB) levels at our nation's recreational beaches is important to effectively managing coastal resources. Described herein is the development and application of an unsteady, three-dimensional hydrodynamic fate and transport model constrained using easily measurable environmental variables such as electrical conductivity (EC) and turbidity. The model was able to simulate observed *Escherichi coli* (*E. coli*) concentrations at three beaches in close proximity to the Burns Waterway along the Indiana Dunes National Lakeshore. This model utilized an unstructured grid that has the ability to accurately represent local features in the area, including the complex shoreline and breakwaters that influence hydrodynamics and mixing. This allows for the better prediction of FIB at local beaches, reducing human health risks and decreasing the number of unnecessary beach closures.

To my family.

ACKNOWLEDGEMENTS

I would like to thank my advisor Dr. Mantha S. Phanikumar for his guidance, knowledge, and insight that helped me complete my thesis. I would like to thank my committee members, Dr. Shu-Guang Li and Dr. Irene Xagoraraki, for their assistance and feedback.

I would like to thank Dr. Pramod Thupaki for his patience, support, and help with the FVCOM program, providing knowledge in the areas I was lacking. Without him I would have been very challenged to complete all of my research objectives. I would also like to thank my friend and colleague, Tuan D. Nguyen, for the numerous discussions leading to the completion of my thesis.

Lastly, I would like to thank my family for the love and support they provided during this entire process. My family is the reason why I have achieved all that I have and without them I wouldn't be the man I am today.

TABLE OF CONTENTS

LIST OF TABLES

LIST OF FIGURES

CHAPTER 1

1.1 Introduction

One of the major indicators of decreased surface water quality is the increased presence of fecal indicator bacteria (FIB), such as *Escherichia coli* (*E. coli*), within the water column. While most *E. coli* are harmless, they are defined as FIB because they are an easily measured quantity and can indicate the presence of health risks to humans. Since human interaction with surface water most often occurs in the near-shore regions, FIB concentrations have become an essential measurable quantity examined at many recreational beaches. For example, for water to meet recreational standards in the State of Indiana, the *E. coli* concentration must be less than 235 colony-forming units (CFU) per 100 mL for any one sample with a geometric mean of less than 125 CFU/100 ml for an entire month (National Parks Service, 2014). However, measurement of FIB concentrations contained in water samples requires approximately 18-24 hours to complete the assays, making it difficult to identify when water quality advisories should be posted. Currently, when a water sample is found to have a FIB concentration greater than 235 CFU/100 ml, the corresponding beach advisory is posted the following day and samples are continually run each day until the beach FIB concentrations are below recreational standards (National Parks Service, 2014).

The introduction of *E. coli* can come from many known sources, including storm and sanitary sewers, natural rivers, surface runoff, animal and shorebird populations, and groundwater discharge (McLellan, 2004). There are many variables that influence the fate and survival of *E. coli* within a specific location, including the turbidity of the water, intensity of sunlight, and the magnitude and direction of the water currents (Francy et al., 2013). As computational technology has become more readily available, numerical models have been developed to simulate these interactions to better predict *E. coli* concentrations and to address the management of coastal regions.

Currently hydrodynamic model parameters are constrained by the model's ability to simulate observational current data. Observational current data can be obtained in many different ways, but the most common method today is to utilize current measurements from an Acoustic Doppler Current Profiler (ADCP) deployed at a specific location, measuring the current magnitudes and directions at defined depth intervals throughout the water column. However, because of the cost of ADCP units and the necessity for accurate data, they are most often deployed in regions where human activities will not impact them, often resulting in deployments in deep water, far from the near-shore region. While deep-water ADCP observational data is adequate to test the accuracy of a model's lake-wide hydrodynamics, they are deficient in the ability to verify near-shore hydrodynamics and transport.

Tracer studies in the near-shore region can be used to reduce the uncertainty in mixing parameters, which are needed to model solute transport accurately. However, tracer studies are expensive and time consuming; therefore, the use of easily-measurable environmental parameters may be more attractive to constrain transport model parameters. An analysis is to be conducted that focuses on these near-shore hydrodynamic interactions, utilizing an unsteady, unstructured, three-dimensional, hydrodynamic transport model. The analysis will focus on further constraining the hydrodynamic and mixing parameters by using easily measurable near-shore environmental variables, such as electrical conductivity (EC) and turbidity, and applying those parameters to an *E. coli* transport model to obtain an accurate near-shore *E. coli* model.

1.2 Objective

The objective of this research is divided into three parts: (a) constraining hydrodynamic and transport models using environmental variables, (b) using the constrained model to simulate *E. coli* concentrations in the water column, and (c) comparing an unstructured grid model to a structured gird model. The constraint placed on the hydrodynamic and transport model will be its ability to simulate EC at the three sample sites in close proximity to a waterway's outfall. This analysis will utilize an unstructured grid to capture the near-shore hydrodynamic interactions in an attempt to improve existing hydrodynamic and transport models. Model performance metrics will be used to determine the quality of the hydrodynamic model produced. From the performance metrics, the goal is to provide insight into the use of EC as a parameter to constrain hydrodynamic models. After the hydrodynamic/transport parameters are constrained, the model will be coupled with an *E. coli* model to simulate *E. coli* concentrations in the near-shore region. Model performance metrics will be computed to summarize the *E. coli* model's ability to simulate observed *E. coli* concentrations and then compared to previous models to determine its accuracy. From this analysis, the goal is to provide insight into the use of an unstructured grid and the use of the specified water quality parameters to estimate *E. coli* concentrations in the near-shore region.

The coupled hydrodynamic and *E. coli* models will also be used to examine the relationship between the measured turbidity in the near-shore region with the simulated *E. coli* concentrations. After examining the relationship between these two parameters, it can be determined if the use of a sediment-transport model is essential to the modeling of *E. coli* levels that are above recreational standards or if a water quality model without sediment-transport is sufficient in simulating *E. coli* concentrations. A graphical view of the process used to investigate the objectives is shown in Figure 1.

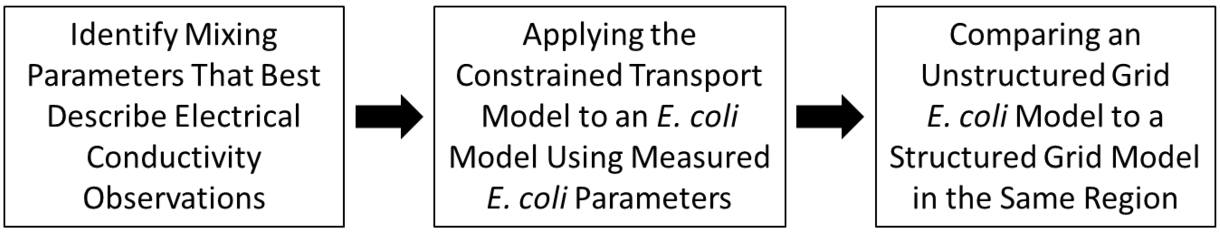

Figure 1: Flow chart of the investigation

1.3 Motivation

The goal of this analysis is to better constrain hydrodynamic and transport models using easily measureable environmental variables. One of the largest sources of uncertainty in near-shore transport models is associated with mixing parameters and this uncertainty propagates into *E. coli* fate and transport models as well. Every near-shore region is unique and has different properties that impact the hydrodynamics differently. The main method used to accurately quantify transport at this time is a dye tracer study. However, these studies are time consuming, labor intensive, and in most cases only capture the transport characteristics for a short period of time. Utilizing easily measurable environmental variables within the water column as a tracer allows for hydrodynamic and transport data to be obtained inexpensively and for long periods of time, in order to accurately constrain mechanistic models. These constraints can be easily applied at any location as long as there are no unknown sources that contribute to the loss/gain of the EC within the domain, allowing for more accurate transport models.

1.4 Literature Review

Hydrodynamic models have been employed to model a wide range of near-shore systems throughout the world, ranging from those interacting with oceans to those interacting with inland lakes. These models have utilized a variety of grids and numerical methods in an attempt to accurately simulate the natural hydrodynamics. Coupling these hydrodynamic models with transport models has allowed investigators to identify contaminant sources and predict future contaminant concentrations in near-shore regions. As computational power has become more accessible, an increased number of mechanistic models have been created to simulate hydrodynamics in near-shore regions. Consequently, after these models were created they were compared with observational data to ensure their accuracy.

In an attempt to validate a lake-wide transport model, an analysis employed EC as a conservative tracer and recorded the measurements of EC at various locations throughout the body of water in a four km long lake, with an average depth of 4 m in Berlin, Germany. This model utilized a two-dimensional, finite-difference grid, with grid resolutions ranging from 10-150 m and harnessed the increased EC introduced to the lake from two inflow rivers as boundary conditions for the model (Schimmelpfennig et al., 2012). The model was able to successfully predict EC throughout the lake (Schimmelpfennig et al., 2012). An important aspect of this study was the application of EC as a conservative tracer, to test mechanistic lake-wide transport models. It was also shown that EC performed better as a tracer than water temperature, another naturally occurring measurable quantity within a water body (Schimmelpfennig et al., 2012).

Another model verification process was analyzed on a more comprehensive level to ensure accurate hydrodynamic modeling. This analysis utilized a three-dimensional, structured, finite-difference, nested model to capture the large-scale lake-wide circulation, while also capturing the small-scale near-shore circulation. Magnitudes and directions of water currents were measured using bottom-mounted, upward-looking ADCP at five different locations in close proximity to Burns Waterway for a period of 40 days (Thupaki et al., 2013a). A continuous-release dye study was also conducted to observe the plume evolution and obtain breakthrough data at three local beaches, while also measuring a mean horizontal dispersion coefficient to further constrain the transport model (Thupaki et al., 2013a). Utilizing the five observational data points for water velocity and the measured mean horizontal dispersion coefficient, the hydrodynamic and transport models were constrained on a very comprehensive level. It was found that the model was able to simulate the mean velocity field and energy contained in the larger scales of motion (lake-wide), but the model significantly under-estimated the energy in the smaller scale, near-shore region. This showed that different methods should be utilized to validate near-shore hydrodynamic models other than ADCP-data.

Attempts to verify hydrodynamic models on both large and small scales have led to the use of these models, coupled with fate and transport models, to determine the sources of contamination in the near-shore region. A study was conducted on the island of Oahu, in Hawaii, in order to settle a dispute between the Sierra Club and Hawaii's Thousand Friends against the city and county of Honolulu (Connolly et al., 1999). The plaintiffs argued that the city and county were violating the Clean Water Act (CWA) because of the discharge from the Sand Island Wastewater Treatment Plant. A 3-D, time-dependent coastal ocean circulation model was applied to the entire island of Oahu, utilizing grid cells ranging from 400 m to 4 km. The model utilized observational *E. coli*, Enterococci, and *C. Perfringens* values at five recreational beaches on the island. Prior to this study, there had not been a comprehensive coastal water quality assessment of this size (Connolly et al., 1999). An important aspect of this study was its ability to show that water quality parameters could be modeled successfully on a large scale. The study was also able to identify multiple sources of *E. coli* and determine the contribution of each to the decreased water quality values at the local recreational beaches. The results of the study indicated that a large portion of the pathogenic organisms affecting the recreational beaches did come from the wastewater treatment plant; however, another major source was identified, a local canal. The study also reported an implied relationship between indicator organism counts at the eastern beaches within the canal and rainfall in the region.

Studies were also conducted on the West Coast marine beaches (i.e., high salinity), in an attempt to determine the sources of FIB in the water (Ho, 2011). Nine different ADCP deployments were used for this study, obtaining long-term (~5 months) data at one position and short-term data (~3 days) at three other locations around Avalon Bay, California. An important observation of this study was that anthropogenic activities within the Bay were shown to represent a significant source to the variability in near-shore water quality (Ho, 2011). Utilizing still photos and ADCP deployments, a relationship between boat activity and *E. coli* concentrations along the beach was shown; however, the cause of the relationship was not proven (Ho, 2011). The study predicted that the anthropogenic activities introduced increased shear stress to the sediment layer, increasing the suspended sediments, re-suspending FIB within the water column.

Another West Coast study was performed at Newport Bay in California (Jeong et al., 2005). The objective of their study was to identify the sources of FIB from various marinas near Newport Bay. The study utilized thousands of water samples (n = 4132) in close proximity of two marinas in Newport Bay. It was shown that both dry weather and wet weather runoff had a significant impact on the FIB concentrations in the two marinas (Jeong et al., 2005). In fact, it was found that the FIB concentrations at the two marina locations were fairly homogeneous, indicating that a common source existed between the two marinas, large-scale runoff, from non-point sources (Jeong et al., 2005). The study determined that long-term strategies for treating non-point sources would be more advantageous than targeting point sources because of the high impact that the non-point sources had on the FIB concentrations near Newport Bay (Jeong et al., 2005).

A number of other studies have been performed in the Great Lakes region in an attempt to identify FIB sources. A tributary and a large ditch were analyzed in southern Lake Michigan to identify the FIB variation at Mt. Baldy Beach for a period of one month (Liu et al., 2006). This study utilized a two-dimensional, finite-element, structured grid model with resolutions approximately 1-2 km for the whole lake and about 100 m near-shore. An overall first-order inactivation coefficient of 0.5 – 2.0 per day was used, incorporating a time-dependent inactivation rate by temperature, sedimentation, and observed solar insolation (Liu et al., 2006). This study provided evidence that the tributary and ditch surrounding the beach were major contributors to the *E. coli* contamination at the beach while also indicating that other sources of *E. coli* may have existed in the area of interest.

Another analysis was performed along a 72 km shoreline of Lake Michigan, using two known point sources (rivers) to perform a budget analysis of *E. coli*. This analysis utilized a three-dimensional, finite-difference, nested model to capture the large-scale lake-wide circulation while also capturing the small-scale near-shore circulation. An important aspect of this study was that it showed that solar inactivation had a greater impact on the *E. coli* loss rates than the settling of the particles, but that dilution due to advection and diffusion had the greatest effect on the net loss of *E. coli* (Thupaki et al., 2010). While, this study did indicate a relationship between bottom shear stresses and *E. coli* peaks, the relationship was not studied.

Thupaki et al., (2013b) incorporated a sediment-transport model into a three-dimensional, finite-difference, structured, nested model to analyze the significance of sediment-transport on *E. coli* concentrations and to better predict *E. coli* concentrations. The analysis was performed on the southern shoreline of Lake Michigan, near Burns Harbor, for a period of approximately 40 days. The study was able to quantitatively determine the importance of sediment re-suspension on the *E. coli* concentrations within the water column. It was observed that the addition of the sediment-transport model to the hydrodynamic model provided significant improvement to the model's prediction of *E. coli* concentrations (Thupaki et al., 2013b). It was concluded that re-suspension of *E. coli* from the bottom sediment was an important process in relation to near-shore water quality (Thupaki et al., 2013b).

The present analysis being performed in the near-shore region, along the Indian Dunes Lakeshore, is directly related to the previously mentioned studies; however, this analysis is unique because it attempts to use EC values to constrain the transport parameters within the near-shore region, and then applies the constrained transport characteristics to an *E. coli* model to better predict the FIB concentrations at local recreational beaches. This analysis also utilizes an unstructured grid, which has yet to be applied to Lake Michigan at the time of this study.

CHAPTER 2

2.1 Study Area

Lake Michigan is a unique body of water located within the continental United States. It is the fifth largest freshwater lake by surface area in the world (58,000 km^2) and the seventh largest by volume, encompassing 4,920 km^3. The lake is surrounded by four states: Michigan, Illinois, Wisconsin, and Indiana, with its deepest point at about 300 m (Figure 2). The lake is utilized commercially for drinking water, fishing, and as a mode of transport for goods, while also providing numerous recreational beaches to local communities. Consequently, the wide variety of demands on the lake and its economic impact to local communities has led to increased water quality awareness.

Figure 2: Lake Michigan and surrounding land masses

The near-shore region investigated consisted of three recreational beaches: Ogden Dunes Beach 1 (OD1), Ogden Dunes Beach 2 (OD2), and Ogden Dunes Beach 3 (OD3), near Burns Waterway, along the Indiana Dunes National Lakeshore (Figure 3). The land to the east of Burns Waterway is used for commercial purposes and the land to the west of Burns Waterway is used for recreational purposes. The recreational beaches' water quality is of concern because of their known increased FIB concentrations. For example, Indiana beaches along southern Lake Michigan rank 24th (out of 30 states) for beach water quality (Beaches, 2014). It is thought that the water quality at the three beach locations is significantly impacted by Burns Waterway (Thupaki et al., 2013b).

Figure 3: Near-shore region of interest

2.2 Current Data

The method for measurement of water currents has come a long way since the beginning of observational oceanography. Primitive measurement tools include bucket wheels that were used to calculate the velocity of the water by the number of rotations for a defined period of time; however, bucket wheels required a person to count every rotation, which is not feasible for long periods of time. Primitive bucket wheels were eventually replaced by velocity meters that used a propeller and the rotations were counted electronically; however, these meters needed constant maintenance to ensure accurate measurements, making long-term deployments difficult. Lagrangian drifters were developed to float on the surface of the water while collecting their GPS locations to calculate the velocity between multiple locations; however, drifters were limited to the top-most layer and unable to determine velocities throughout the water column. ADCPs were developed allowing for the measurement of water velocities throughout the water column at any given location. ADCPs transmit and receive sounds waves at a known frequency from the water column, allowing them to calculate the fluid velocity (scalar) in the water column based on the Doppler shift principle. Utilizing multiple transmitters allows the ADCPs to calculate the fluid velocity in multiple directions (vector). Utilizing reliable and compact data storage methods allows for ADCPs to be deployed for long periods, capturing the flow velocities throughout the water column.

A single, upward-facing 600kHz RDI-Monitor ADCP (Figure 4) was deployed approximately 9 km from the study site (41.71059 N, 87.20996 W), at a depth of ~20 m, to collect observational data for water velocities in the x, y, and z directions (Figure 5). The deployment lasted from May to September 2008 to capture an extensive observational dataset. The ADCP was programmed to utilize a ping rate of 0.1 Hz and the data was ensemble—averaged every five minutes. The ADCP was programmed so the predicted standard deviation of the measurements was less than 0.1 cm sec^{-1} (Teledyne, 2006). The RDI Workho32rse Monitor ADCP was serviced on August 5, 2008, to replace the on-board battery.

Figure 4: Example of ADCP experimental setup.

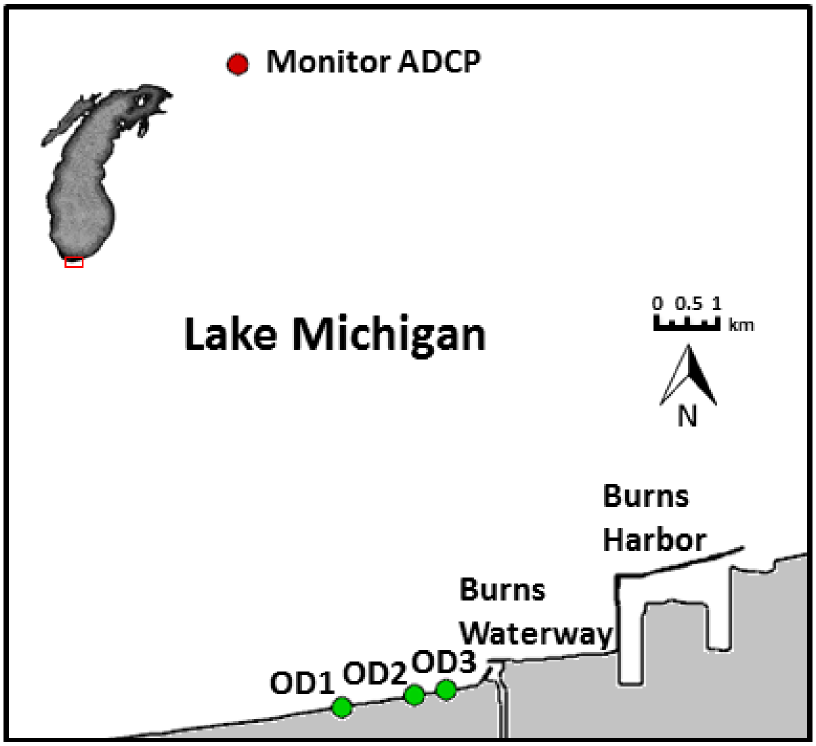

Figure 5: ACDP deployment location in relation to the area of interest.

2.3 *E. Coli* Data

Water samples were taken at OD1, OD2, and OD3 beach locations and at the Burns Waterway USGS Gauge (#04095090) location to evaluate the ability of the model to simulate the observational *E. coli* concentrations at the Ogden Dunes beach locations. The water samples were taken twice daily (morning and afternoon) from June 9–August 28 in 2008. The water samples were collected from knee-deep water and analyzed for *E. coli* at the USGS Great Lakes Science Center in Porter, Indiana, using membrane filtration methods according to section 9222G, APHA (1998). As described in Liu et al. (2006) the membrane filters were incubated on mFC agar at 44.5 C° for 24 hours, transferred to EC-MUG agar (Difco, 222200), and incubated for 24 hours at 44.5 C°. Individual colonies that produced florescence under a long wavelength (366-nm) ultraviolet light were considered *E. coli*, reported in CFU/100 mL.

Both light-bag and dark-bag experiments were conducted during the sampling period when the water samples were taken. The tests provided an estimate of the sunlight extinction coefficient and light-based inactivation rate of the *E. coli* in the region. As described in Ge et al. (2012b) the tests were constituted using 530 mL darkened and 200 mL transparent WhirlPak bags that contained freshly collected water from Lake Michigan and were conducted on a typical sunny day in June 2008. After the light-bag and dark-bag samples were created, all the samples were placed in coolers on ice, held at 4 C°, and analyzed using the Colilert-18 method four hours after collection. The base mortality coefficient, k_d, was calculated to be 0.55 d^{-1} and the solar inactivation rate, k_I, was determined to be approximately 0.00301 m^2 W^{-1} d^{-1}.

2.4 Electric Conductivity Data

EC values were measured twice daily (morning and afternoon), using a standard YSI EC probe (www.ysi.com), from June 9 – August 28 at the Ogden Dunes beach locations to validate the simulated EC values obtained from the model. EC measurements were also taken with the same frequency and duration at the Burns Waterway USGS Gauge (#04095090) to act as a boundary condition for the model.

2.5 Turbidity Data

To compare the relationship between turbidity and *E. coli*, turbidity measurements were taken twice daily (morning and afternoon) from June 9 – August 28 at the Ogden Dunes beach locations. The turbidity was measured using a YSI sonde (model 6600).

2.6 Numerical Model

Various mechanistic models have been developed to simulate water circulation. Those models either utilize the finite-difference method or the finite-element method. The finite-difference method is the most basic and is advantageous because of simple coding and computational efficiency. However, this method is unable to capture complex near-shore structures and other features. The finite-element method is advantageous because of its ability to capture these near-shore structures, but is more difficult to code and may be less computationally efficient.

The model employed by this research was the Finite-Volume Community Ocean Model (FVCOM) originally developed by Chen et al. (2003). FVCOM combines the advantages of both the finite-different and the finite-element models, by discretizing the integral form of the governing equations so that it is relatively easy to code and computationally efficient, while also allowing the use of an unstructured grid.

2.6.1 Computational Grid

The graphical user interface (GUI), Surface-water Modeling System (SMS) by Aquaveo (2014), was utilized to create an unstructured grid. The grid was able to capture the local features near Burns Waterway's outfall more accurately using a resolution of approximately 40 m (Figure 6), while also utilizing grid resolutions of approximately 2-5 km for the rest of Lake Michigan (Figure 7). To ensure accurate numerical calculations, a smooth transition from the increased grid resolution to the decreased grid resolution must be achieved and is verified in Figure 8. The grid was constrained to the south at 42.61 N Latitude, 46.13 N Latitude at the north, 84.76 W Longitude in the west, and 88.04 W Longitude in the eastward direction. The computational grid was made up of 12,684 nodes and 23,602 elements.

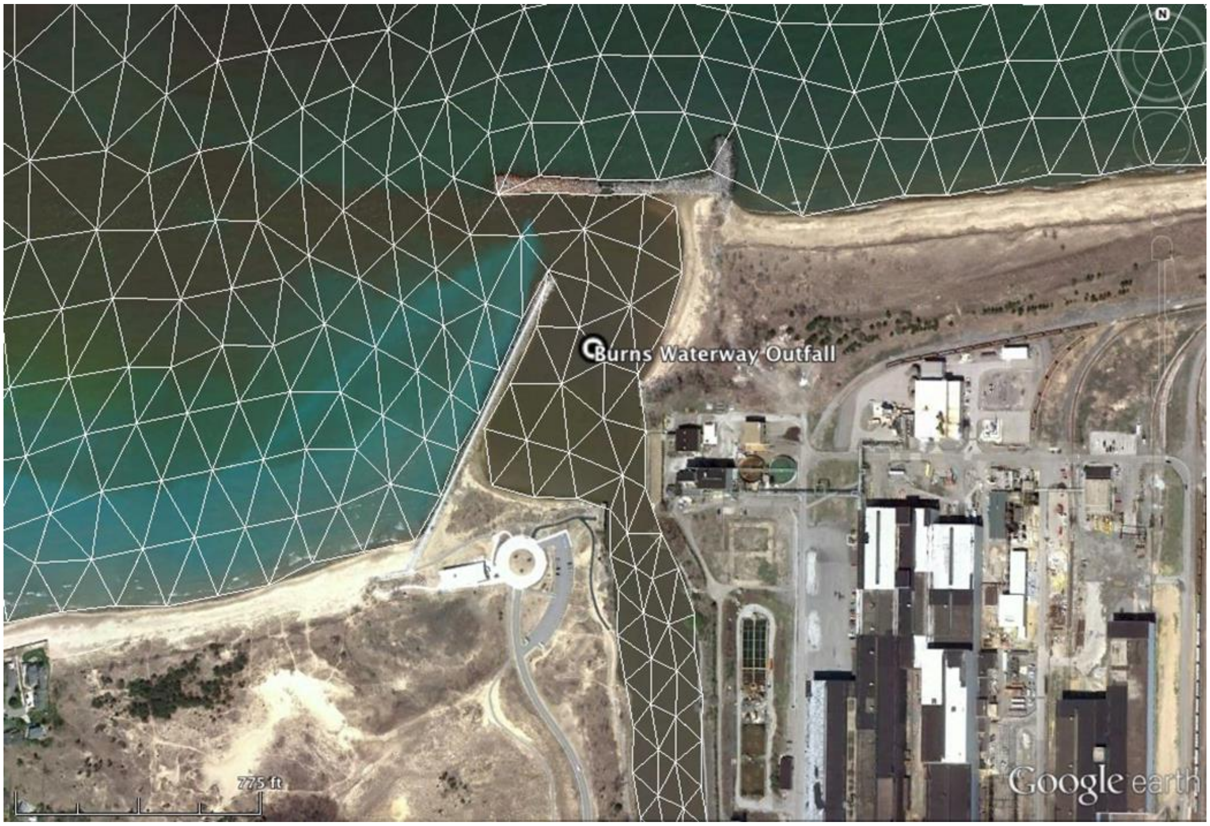

Figure 6: Computational grid showing local features near Burns Waterway outfall using a 40 m grid resolution.

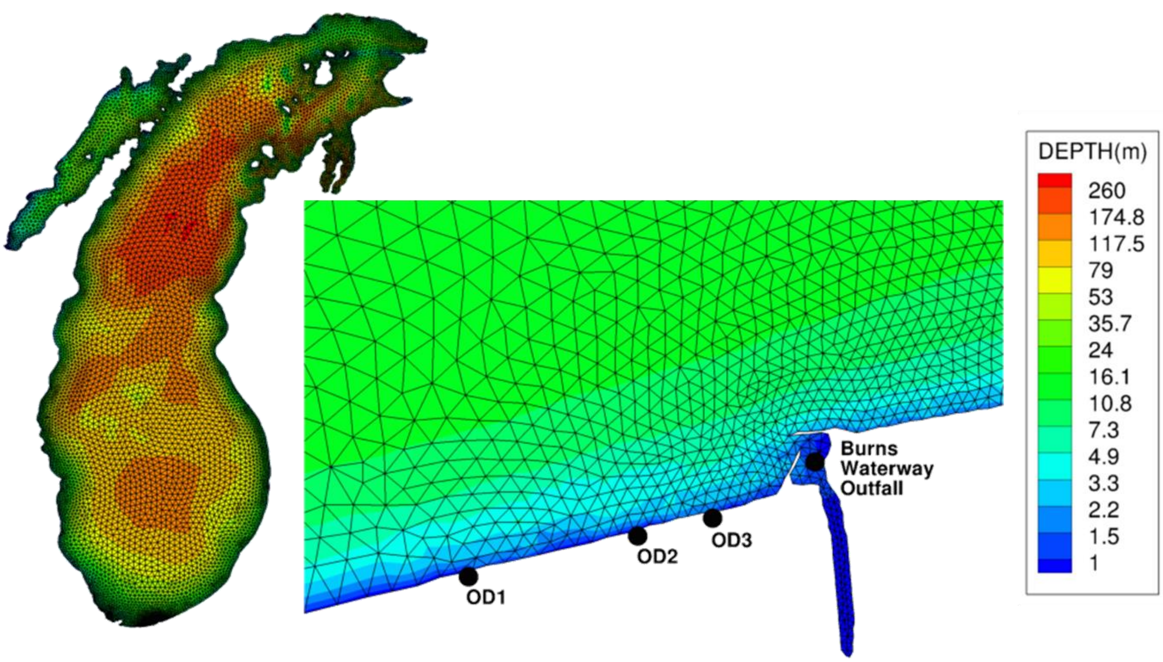

Figure 7: Grid resolution and bathymetry for the lake-wide and near-shore regions.

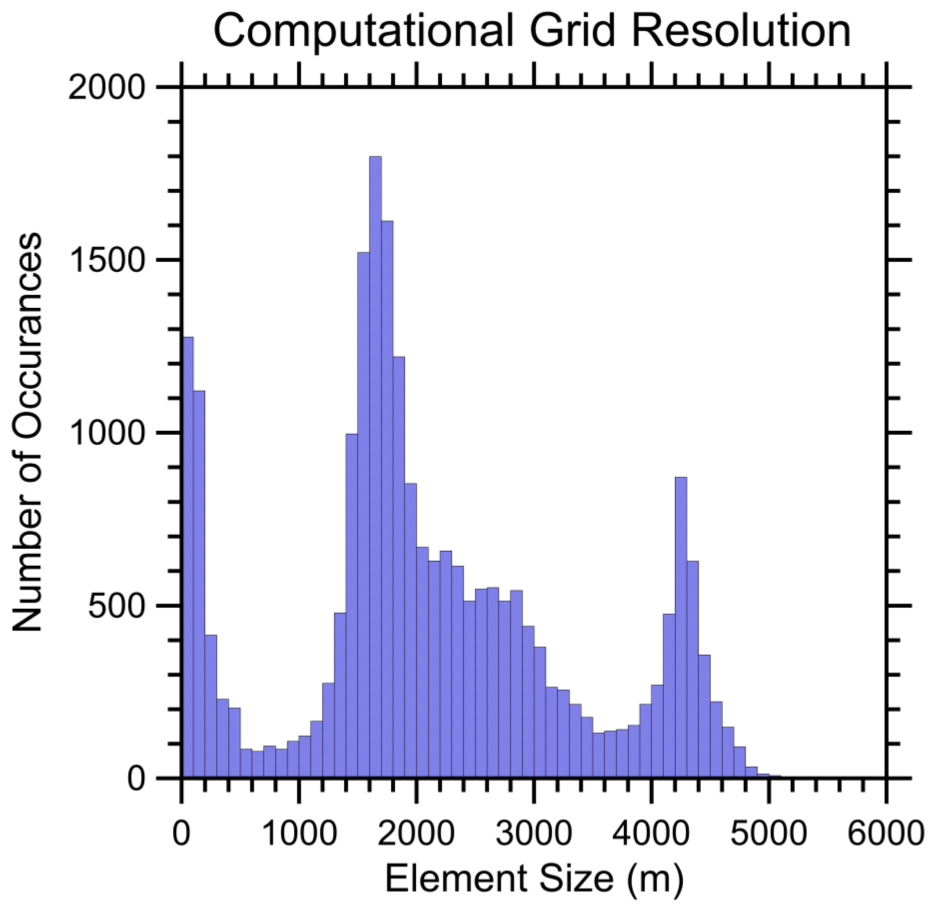

Figure 8: A histogram of grid sizes used in the unstructured grid model

To evaluate the hydrodynamics and mixing properties of the water column, bathymetry values were interpolated to the grid nodes using Matlab R2012a (2012). Two data sets were combined to obtain accurate data. The first data set was obtained from the National Oceanic and Atmospheric Administration (NOAA) Lake Michigan 2008 LIDAR data set along the Indiana coast, utilizing a horizontal resolution of approximately 2 m. This data set was utilized to ensure accurate depth interpolations in the near-shore region where the hydrodynamics and mixing properties are greatly influenced by the water depth. A second data set was obtained from NOAA for the remaining area of Lake Michigan with a horizontal resolution of approximately 90 m.

2.6.2 Currents

Circulation throughout Lake Michigan can be modeled using basic hydrodynamic equations derived from the Reynold's averaged form of the Navier-Stokes equations for continuity (Equation 1) and momentum (Equations 2 and 3) in the x-y directions. The momentum equation in the z-direction can be simplified further to its hydrostatic form (Equation 4). The model utilized 20 vertical (sigma) layers over the water column depth. Because of the Boussinesq approximation, density is assumed constant except when multiplied by gravity.

$$\frac{\partial u}{\partial x} + \frac{\partial v}{\partial y} + \frac{\partial w}{\partial z} = 0 \tag{1}$$

$$\frac{\partial u}{\partial t} + u\frac{\partial u}{\partial x} + v\frac{\partial u}{\partial y} + w\frac{\partial u}{\partial z} - f_v = \frac{1}{\rho_o}\frac{\partial P}{\partial x} + \frac{\partial}{\partial x}\left(2A_M\frac{\partial u}{\partial x}\right) + \frac{\partial}{\partial y}\left[A_M\left(\frac{\partial u}{\partial y} + \frac{\partial v}{\partial x}\right)\right] + \frac{\partial}{\partial z}\left(K_{VM}\frac{\partial u}{\partial z}\right) \tag{2}$$

$$\frac{\partial v}{\partial t} + u\frac{\partial v}{\partial x} + v\frac{\partial v}{\partial y} + w\frac{\partial v}{\partial z} - f_u = \frac{1}{\rho_o}\frac{\partial P}{\partial y} + \frac{\partial}{\partial y}\left(2A_M\frac{\partial v}{\partial y}\right) + \frac{\partial}{\partial x}\left[A_M\left(\frac{\partial u}{\partial y} + \frac{\partial v}{\partial x}\right)\right] + \frac{\partial}{\partial z}\left(K_{VM}\frac{\partial v}{\partial z}\right) \tag{3}$$

$$\frac{\partial P}{\partial z} = -\rho g \tag{4}$$

The variables *x*, *y*, and *z* are the flow directions, *u*, *v*, and *w* are the mean flow velocities in their respected direction, ρ and $\rho_o$are the local and reference density respectively and A_M and K_{VM} are the diffusivity terms in the horizontal and vertical directions for the momentum equations. f denotes the Coriolis paramter, introduced to account for the rotation of the earth, and g is the gravitational acceleration.

Temperature transport is modeled using a scalar transport equation (Equation 5) where T is the temperature of the water, S_T represents the sources and sinks for temperature, and A_H and K_V are the eddy diffusivity in the horizontal and vertical directions respectively for the transport equation.

$$\frac{\partial T}{\partial t} + u\frac{\partial T}{\partial x} + v\frac{\partial T}{\partial y} + w\frac{\partial T}{\partial z} = \frac{\partial}{\partial x}\left(A_H\frac{\partial T}{\partial x}\right) + \frac{\partial}{\partial y}\left(A_H\frac{\partial T}{\partial y}\right) + \frac{\partial}{\partial z}\left(K_V\frac{\partial T}{\partial z}\right) + S_T \tag{5}$$

Boundary conditions affecting water currents and temperature were applied to the hydrodynamic and transport equations utilizing observational metrological data. The meteorological observations were obtained from both the National Climatic Data Center (NCDC) and the National Data Buoy Center (NDBC) weather monitoring stations, at 44 locations surrounding Lake Michigan (Figure 9). Direct meteorological observations that were utilized included wind speed and direction, air temperature, and cloud cover. Long-wave solar radiation was calculated using the model presented by Parkinson and Washington (1979) utilizing air temperature and cloud cover. Short-wave solar radiation was calculated using the clear-sky value (Office, 1971) and the measured cloud cover.

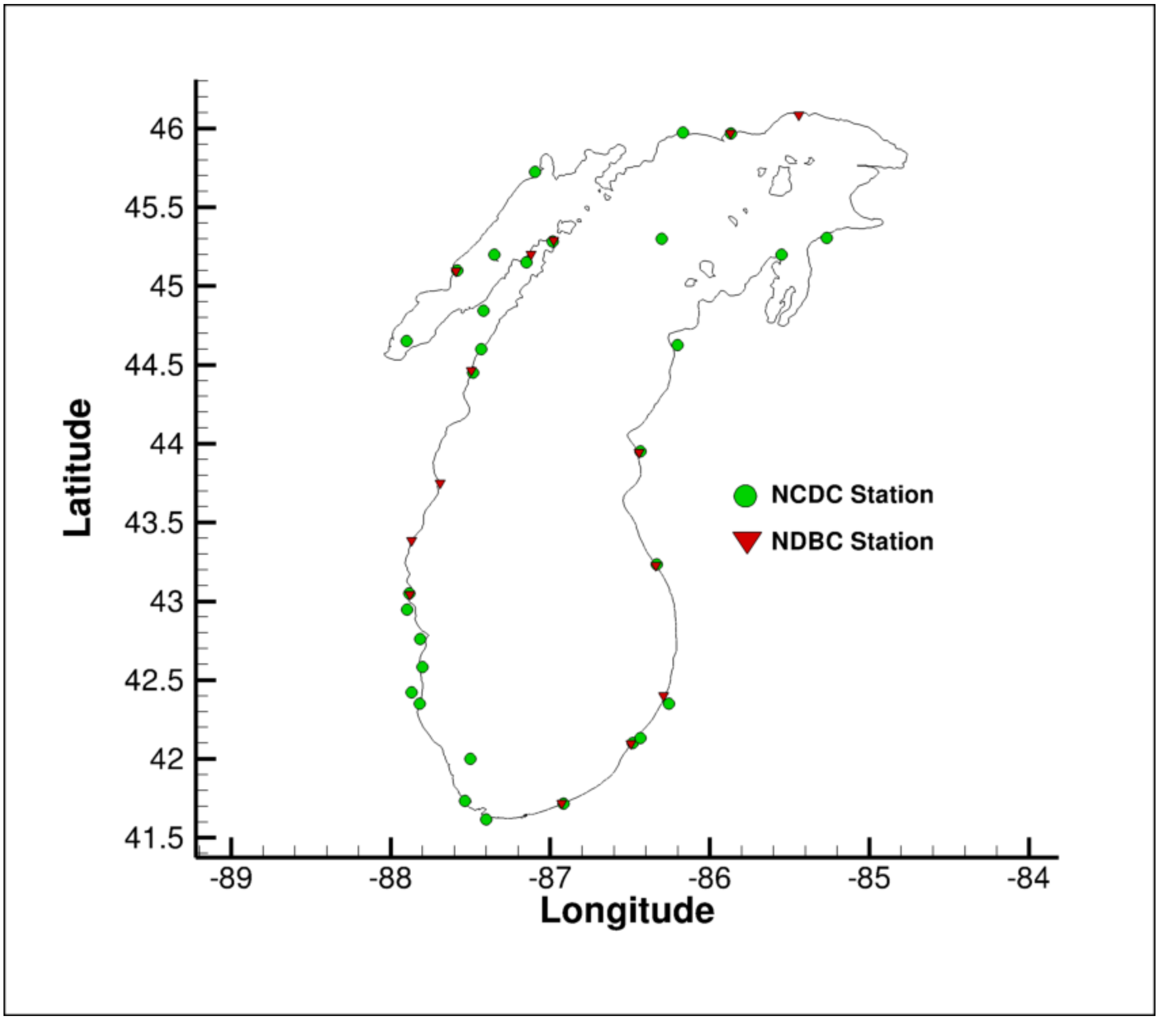

Figure 9: Locations of weather stations utilized surrounding Lake Michigan

To complete the hydrodynamic and transport equations (Equations 1-5), A_M and A_H must be described. The horizontal eddy diffusivity term is calculated using the Smagorinsky eddy viscosity model shown in Equation 6 (Smagorinksy, 1963).

$$A_M = C\Delta x \Delta y \frac{1}{2}\left|\nabla\vec{V} + \left(\nabla\vec{V}\right)^T\right| \tag{6}$$

The variable C is a non-dimensional constant parameter, and the grid sizes $(\Delta x, \Delta y)$ are both included in the calculation. Equation 6 assumes that the horizontal eddy diffusivity is isotropic and equal in both x and y directions. A_H is related to A_M by Equation 7.

$$P_r = \frac{A_M}{A_H} \tag{7}$$

P_r is the turbulent non-dimensional Prandtl number. FVCOM uses the Mellor-Yamada 2.5 turbulence closure model to describe vertical mixing, K_{VM} and K_V (Mellor and Yamada, 1982).

2.6.3 Water Quality Model

A water quality model was coupled with the FVCOM transport model to simulate the EC and *E. coli* concentrations within the water column. Our primary interest was to simulate the *E. coli* concentrations within the water column; however, the EC concentrations were used to further constrain the parameters used by the transport model to reduce uncertainty in the near-shore fate and transport model.

The *E. coli* transport model solved a similar transport equation presented earlier for temperature (Equation 5) and is shown in Equation 8. However, the *E. coli* transport equation utilizes a net loss rate, *k*, due to inactivation and settling to describe the loss mechanisms (Equation 9).

$$\frac{\partial c}{\partial t} + u\frac{\partial c}{\partial x} + v\frac{\partial c}{\partial y} + w\frac{\partial c}{\partial z} = \frac{\partial}{\partial x}\left(A_H\frac{\partial c}{\partial x}\right) + \frac{\partial}{\partial y}\left(A_H\frac{\partial c}{\partial y}\right) + \frac{\partial}{\partial z}\left(K_V\frac{\partial c}{\partial z}\right) + kc \tag{8}$$

$$k = -\left(\frac{f_p v_s}{\Delta z_i} - \frac{f_p v_s}{\Delta z_{i-1}} + k_I I_o(t)e^{-k_e z} + k_d\right)\theta^{T-20} \tag{9}$$

The variable f_p is the faction of *E. coli* attached to particles, v_s is the settling velocity of the particles, Δz_i and Δz_{i-1} represent the thickness of each layer, k_I is the inactivation rate of *E. coli* due to sunlight, $I_o(t)$ denotes amount of short-wave radiation at the water surface due to sunlight, k_e is the extinction coefficient, k_d is the base mortality rate, and θ^{T-20} is the dependence of the loss rate on temperature using the Beer-Lambert relation.

EC was modeled as a conservative tracer, utilizing the transport equation without the addition of a source or sink term, with concentration depending only on the transport within the water column (Equation 10). EC was considered to be conservative because the boundary condition for EC, Burns Ditch outfall, was assumed to be much larger than all the other sources and sinks affecting the Ogden Beach locations. In other words, the difference between the EC values at the mouth of the river and the ambient lake values provides a clear range of EC values and a strong signal that can be measured and modeled. This may not be the case at all sites.

$$\frac{\partial EC}{\partial t} + u\frac{\partial EC}{\partial x} + v\frac{\partial EC}{\partial y} + w\frac{\partial EC}{\partial z} = \frac{\partial}{\partial x}\left(A_H\frac{\partial EC}{\partial x}\right) + \frac{\partial}{\partial y}\left(A_H\frac{\partial EC}{\partial y}\right) + \frac{\partial}{\partial z}\left(K_V\frac{\partial EC}{\partial z}\right) \tag{10}$$

2.7 Model Performance Metrics

To identify the ability of the model to accurately simulate various aspects of the observed data (EC and *E. coli*), several metrics were employed. The metrics calculated at each observational location were the root mean square error (RMSE), the coefficient of determination (R^2), the percent bias (PBIAS), and the Fourier norm (F_n). The Matlab software (Matlab, 2012) was used with predefined scripts to calculate each performance metric. All of the performance metrics utilizing *E. coli* were calculated using $\log_{10}(E. coli\ concentration)$.

2.7.1 Root Mean Square Error (RMSE)

RMSE is a commonly used error index for model validation that is calculated by determining the mean absolute error between the observed and simulated values (Equation 11). RMSE values have been shown to be a good measure of hydraulic model efficiency because of the variability of the values obtained from hydraulic systems (Legates and Mccabe, 1999). A RMSE value of 0 indicates a perfect fit between the observed and simulated values and values range from 0 to ∞.

$$RMSE = \sqrt{\frac{1}{n}\sum_{i=1}^{n}\left(Y_i^{obs} - Y_i^{sim}\right)^2} \tag{11}$$

2.7.2 Coefficient of Determination (R^2)

The coefficient of determination describes the ability of the model to simulate the variance in the measured data (Equation 12). R^2 values range from 0 to 1, with 1 indicating the model does a perfect job describing the model and 0 indicating the model was not able to describe any of the variance in the observed data. Although R^2 is a commonly used statistical term, it has been shown to be over-sensitive to outliers in the data and insensitive to additive and proportional difference between simulated and observed data (Legates and McCabe, 1999). However, R^2 is still calculated because of its wide range of use for model verification.

$$R^2 = 1 - \frac{\sum_{i=1}^{n}\left(Y_i^{obs} - Y_i^{sim}\right)^2}{\sum_{i=1}^{n}\left(Y_i^{obs} - Y_{ave}^{obs}\right)^2} \tag{12}$$

2.7.3 Percent Bias (*PBIAS*)

Percent Bias measures the average tendency of the model to over-estimate or under-estimate the observed data and is shown in Equation 13 (Gupta et al., 1999). *PBIAS* values range from -∞ to ∞, with 0 being the optimal value. Under-estimation is represented by a negative value, while over-estimation is represented by a positive value, indicating the bias in the model.

$$PBIAS = \left[\frac{\sum_{i=1}^{n}\left(Y_i^{obs} - Y_i^{sim}\right)(100)}{\sum_{i=1}^{n}\left(Y_i^{obs}\right)}\right] \tag{13}$$

2.7.4 Fourier Norm (F_n)

Fourier norm is the relative percentage of variance in the observed data that is not explained by the simulated data as described by Beletsky and Schwab (2001) (Equations 14 and 15). A value of 0 would indicate that the simulated results modeled the observed results with no errors and a value of 1 would indicate that the model was not able to explain any of variances in the observed data.

$$\left\|Y_i^{obs}, Y_i^{sim}\right\| = \left(\frac{1}{n}\sum_{i=1}^{n}\left|Y_i^{obs} - Y_i^{sim}\right|^2\right)^{1/2} \tag{14}$$

$$F_n = \frac{\left\|Y_i^{obs}, Y_i^{sim}\right\|}{\left\|Y_i^{obs}, 0\right\|} \tag{15}$$

CHAPTER 3

3.1 Lake Wide Model Verification: ADCP

Simulated current values from the hydrodynamic model were compared to observational measurements for the summer of 2008. In the near-shore region, along-shore (u') and cross-shore (v') velocities are of more interest than north-south (v) and east-west (u) velocities, so the north-south and east-west velocities were converted to along-shore, cross-shore velocities in relation to the shoreline (Equations 16 and 17).

$$u' = u\cos(21.9°) + v\sin(21.9°) \tag{16}$$

$$v' = u\sin(21.9°) + v\cos(21.9°) \tag{17}$$

Comparisons were made between the observed and simulated (vertically integrated) along-shore and cross-shore velocities and are shown in Figure 10. The RMSE value for the water current comparison was 0.040 m s^{-1}. This measurement was comparable to the work in previous studies, comparing simulated water current velocities to observed ADCP measurements (Table 1). The model demonstrated the ability to simulate lake-wide flow. However, the observed measurements were taken at a location approximately 9 km away from the area of interest. Even though the lake-wide hydrodynamics influence transport in the near-shore region, the transport model still needs to be tested in the near-shore region to verify the transport parameters influenced by the local features in the area of interest.

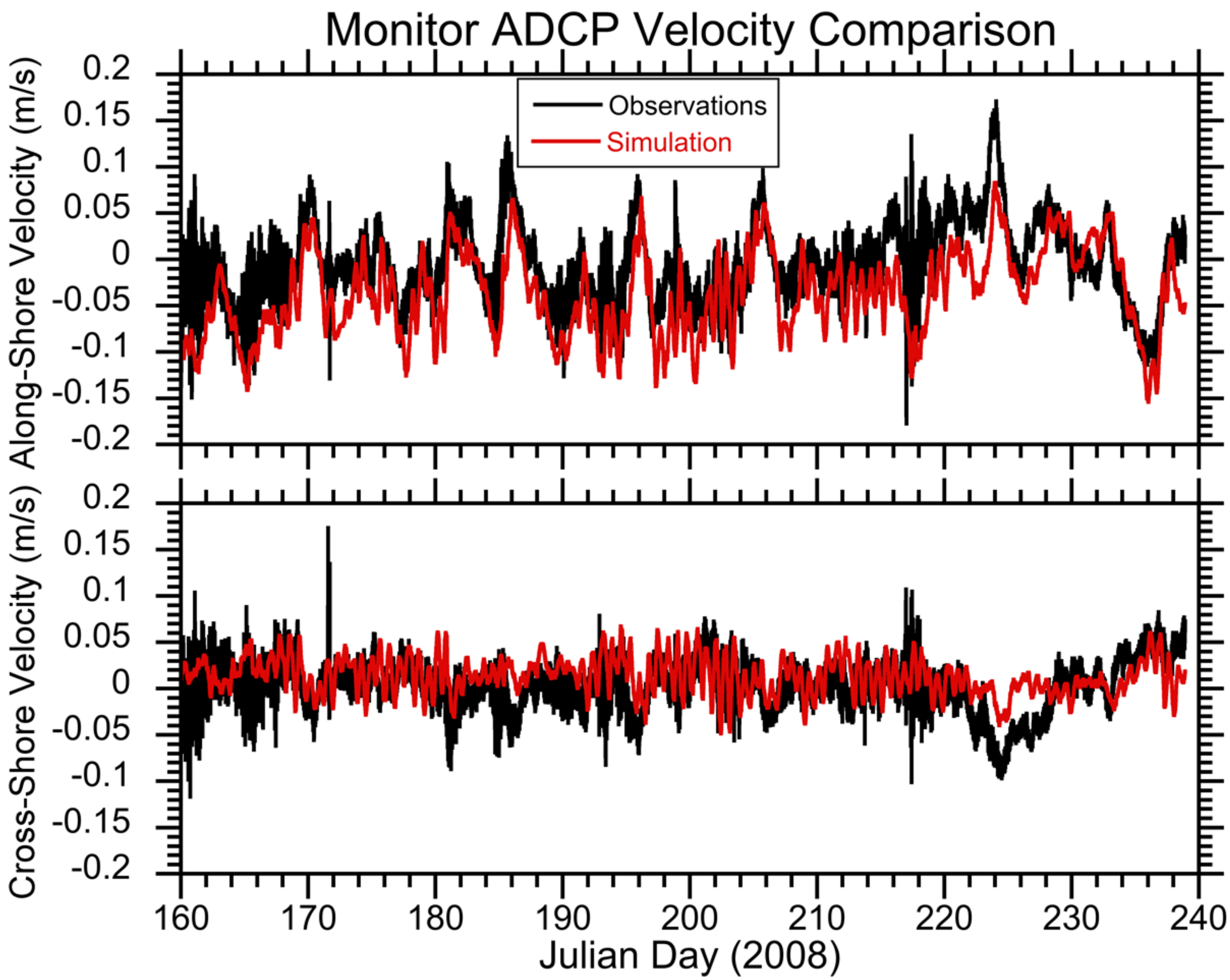

Figure 10: Along-shore and cross-shore, vertically integrated, velocity comparisons with the Monitor ADCP

Table 1: Comparison of water flow velocities with previous investigators

Location	Velocity RMSE (m/s)			Source
	Along-Shore	Cross-Shore	Total	
Lake Michigan (M)	0.048	0.031	0.040	Present Model
North Sea (Lower EMF)	0.060	0.083	--	Grunnet et al., 2004
North Sea (Upper EMF)	0.050	0.108	--	Grunnet et al., 2004
Lake Michigan (M)	--	--	0.031	Thupaki et al, 2013a
Lake Michigan (S)	--	--	0.037	Thupaki et al, 2013a
Lake Michigan (N1)	--	--	0.048	Thupaki et al, 2013a
Lake Michigan (N2)	--	--	0.042	Thupaki et al, 2013a
Lake Michigan (shallow ADCP)	0.030	0.020	0.017	Ge et al., 2012

3.2 Near-Shore Model Verification: Electrical Conductivity

To further examine the transport parameters within the near-shore region, EC measurements were utilized as a conservative tracer. The major ions that affect EC concentrations in lake water include F, Cl, NO_3, SO_4, PO_4, Na, Ca, Mg, and K, leading to many sources and sinks of EC in a natural environment; however, it was assumed that because of the proximity of the three Ogden Beach locations to Burns Waterway outfall (~1 km), no sources and sinks were considered significant when compared to the Burns Waterway outfall boundary condition. EC measurements have also been shown to be dependent on the temperature of the water (Hayashi, 2004); however, the simulated temperature in the near-shore region was shown to be relatively constant between the three sample locations, indicating that an EC-temperature relation was not needed. Even with all of the uncertainty in the EC values in lake water, Schimmelpfenig et al. (2012) concluded that EC could be a suitable tracer. Adjusting the mixing parameters (Table 2), the physics of the model were altered to ensure accurate simulated transport by comparing the simulated (vertically averaged) and observed EC measurements at the three observational beaches (Figure 11) with a background concentration of 286 μmhos/cm. These comparisons are supported by the performance metrics presented in Table 3.

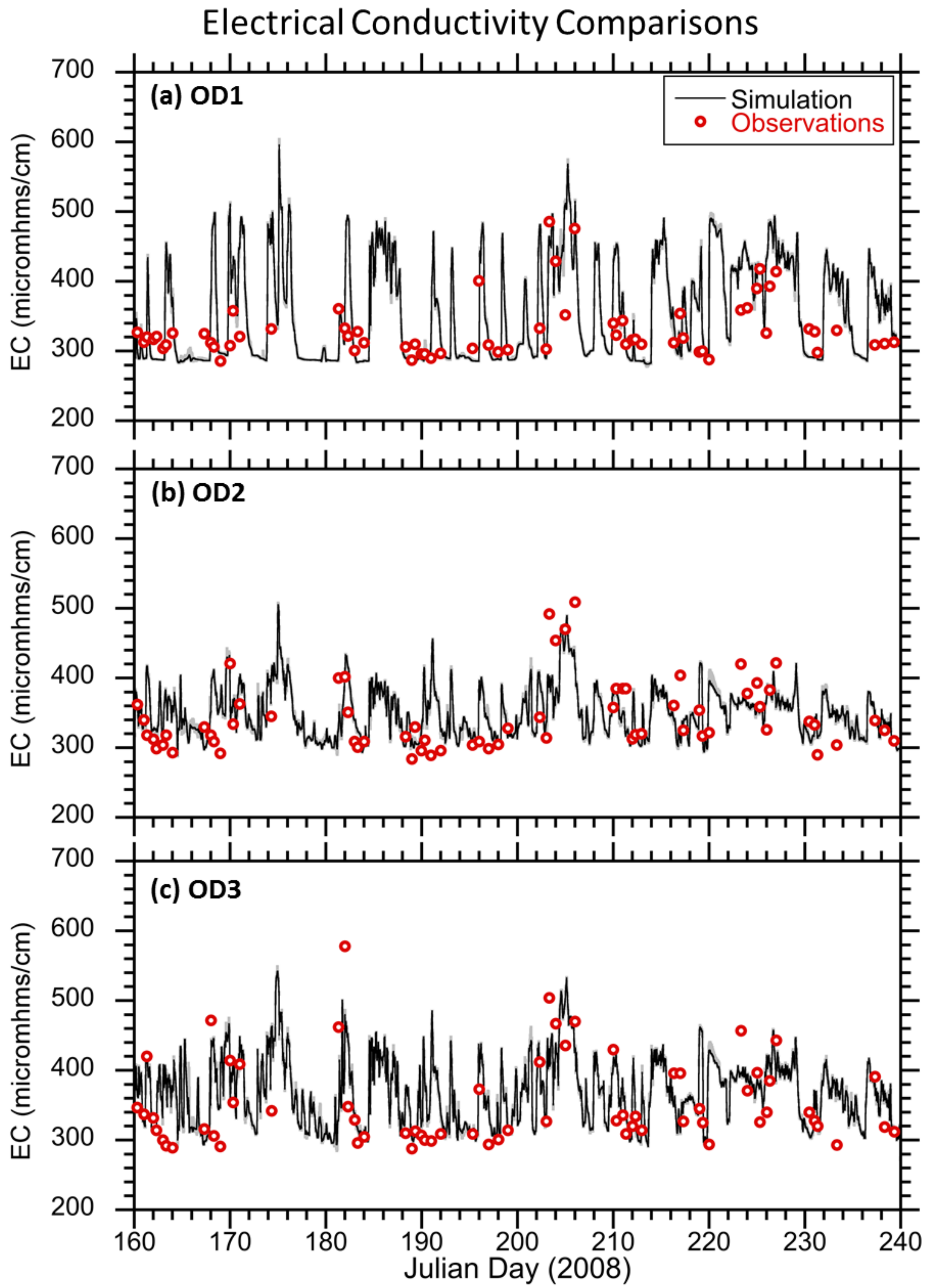

Figure 11: Electrical conductivity plots for observed values compared to the simulated values with the grey-colored bands representing ± 0.5% uncertainty in the chemical measurements at (a) OD1, (b) OD2, and (c) OD3.

Table 2: Mixing flow parameters

Parameter	Value
Horizontal Mixing Coefficient	0.10 m s^{-1}
Vertical Mixing Coefficient	10×10^{-5} m s^{-1}
Horizontal Prandtl Number	10
Vertical Prandtl Number	10

Table 3: Electrical conductivity comparison metrics

Location	RMSE (µmhos cm^{-1})	R^2	PBIAS	F_n
OD1	0.696	0.489	-7.916	0.209
OD2	0.471	0.462	-2.581	0.136
OD3	0.622	0.454	-5.907	0.174

The PBIAS at all three Ogden Beach locations suggests that the model slightly underestimates the EC of the water column (Table 3). However, F_n indicates that the model was able to explain 79.1%, 86.44%, and 82.65% of the variance in the observed values at OD1, OD2, and OD3, respectively, indicating the model fit the observational measurements (Table 3). To further verify the EC transport, the error norms (I_1 and I_2) were calculated to perform a direct statistical comparison to previous studies utilizing EC as a tracer (Equations 18 and 19).

$$I_1 = \frac{1}{n}\left(\frac{\sum_{i=1}^{n}\left|Y_i^{obs} - Y_i^{sim}\right|}{\sum_{i=1}^{n}\left|Y_i^{obs}\right|}\right) \tag{18}$$

$$I_2 = \frac{\sqrt{\sum_{i=1}^{n}\left(Y_i^{obs} - Y_i^{sim}\right)^2}}{\sqrt{\sum_{i=1}^{n}\left(Y_i^{obs}\right)^2}} \tag{19}$$

I_1 is the mean absolute percent error (MA%E) proposed by Mayer and Butler (1993) and I_2 is the RMSE of the model divided by the root mean square of the observed data (RMS_{obs}). The error norms are comparable with the results of the study performed by Schimmelpfennig et al. (2012) in Lake Tegel (Table 4); however, Schimmelpfennig et al. (2012) noted better agreement between model and EC data. This is attributed to the fact that the Lake Tegel measurements were taken outside of the near-shore region, where there is less uncertainty in the mixing of the water column, while also utilizing a 2-D computational grid that does not account for the vertical mixing of the water.

Table 4: Error norms for electrical conductivity models

Location	I_1	I_2	**Source**
OD1	0.149	0.209	Present Model
OD2	0.106	0.136	Present Model
OD3	0.138	0.174	Present Model
Lake Tegel	0.040	0.061	Schimmelpfennig et al., 2012

The performance metrics (Table 3, Table 4) show that the model was able to simulate the tracer concentrations better at OD2 and OD3, the closest beach to Burns Waterway's outfall (< 1 km). As the distance increased from the outfall to the OD1 observational location (> 1 km), the model was less accurate in its ability to simulate the observed data. It is speculated that the Smagorinsky mixing parameterization used in the FVCOM caused excessive damping that contributed to the degradation in model performance at larger distances although waves (ignored in the modeling) and wave-current-interactions are also expected to play a role.

Based on the metrics presented in Table 3, the ability of the model to capture most of the peaks and the low values in the data, the performance of the present near-shore transport model is considered reasonable. The final mixing parameters (shown in Table 2) were then used in the *E. coli* fate and transport model.

A specific near-shore parameter of interest is the horizontal dispersion coefficient (A_H). A_H is the rate of mixing in the near-shore region and has a significant impact on the transport of materials

(Equation 5). The near-shore region was defined as the area from the shoreline to the 15 m isobath (Nearshore, 2009). Using that criterion, the near-shore region for this investigation was estimated to consist of the water approximately 4.5 km away from the area of interest, in all directions. The estimated A_H value in the near-shore region utilizing the "4/3 power law" and a median length scale of 100 m is 0.05 m^2 s^{-1}. However, using the model, the median A_H in the near-shore region was calculated to be 1.96 m^2 s^{-1} and a distribution of the values is shown in Figure 12. The reason that the "4/3 power law" was shown to underestimate the near-shore horizontal dispersion coefficient is thought to be due to its inability to account for wave breaking, wave refraction, and the shear effect between the water currents and the bottom of the lake introduced by the decreased bathymetry in the near-shore region. The calculated A_H value is within the range of measured total dispersion values in the near-shore region by Johnson (2004) between 1.29 and 3.88 m^2 s^{-1}.

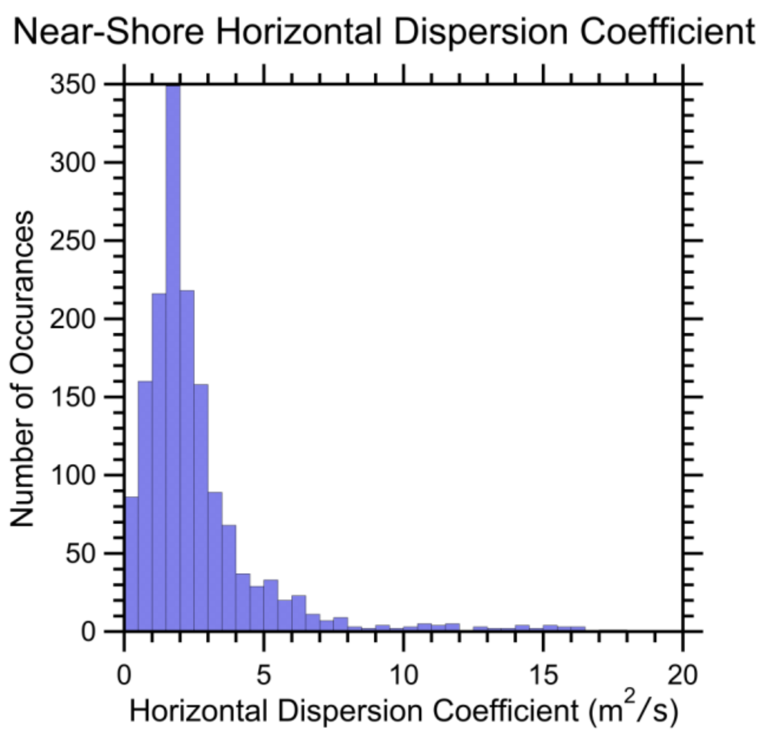

Figure 12: A histogram of the horizontal dispersion coefficient in the near-shore region

3.3 *E. coli* Model

The mixing parameters used to simulate the EC concentration (Table 2) were then used to simulate the *E. coli* concentrations for the near-shore region. The parameters utilized by the *E. coli* model to determine the *E. coli* net loss rate, *k*, are shown in the Table 5. All of the *E. coli* net loss rate parameters were constrained by measured values and values that were shown to be acceptable by previous investigators. The results of the *E. coli* model were compared to the observed values at Ogden Dunes Beach locations (Figure 13). The comparison shows the results of the simulation with a black line and ±50% uncertainty in the biological *E. coli* measurements is shown using a grey band. Turbidity measurements are also displayed by the color of each data point, corresponding to the color bar. An example of the plume evolution is shown in Figure 14 for Julian Day 219, 2008. The model performance metrics are presented in Table 6.

Table 5: Parameters used for *E. coli* model

Parameter	Value	Source
$\boldsymbol{\theta}$	1.07	Epply, 1972
$\boldsymbol{v_s}$	1 m d^{-1}	Based on the Estimates from Eadie, 1997
$\boldsymbol{k_d}$	0.55 d^{-1}	Ge et al., 2012b
$\boldsymbol{k_I}$	0.003 m^2 W^{-1} d^{-1}	Ge et al., 2012b
$\boldsymbol{f_p}$	0.05	Estimate from Thupaki et al., 2013b

Table 6: *E. coli* performance metrics

Location	RMSE (CFU/100 mL)	$\boldsymbol{R^2}$	PBIAS	$\boldsymbol{F_n}$
OD1	0.809	0.380	24.283	0.660
OD2	0.600	0.425	10.489	0.408
OD3	0.647	0.425	6.511	0.408

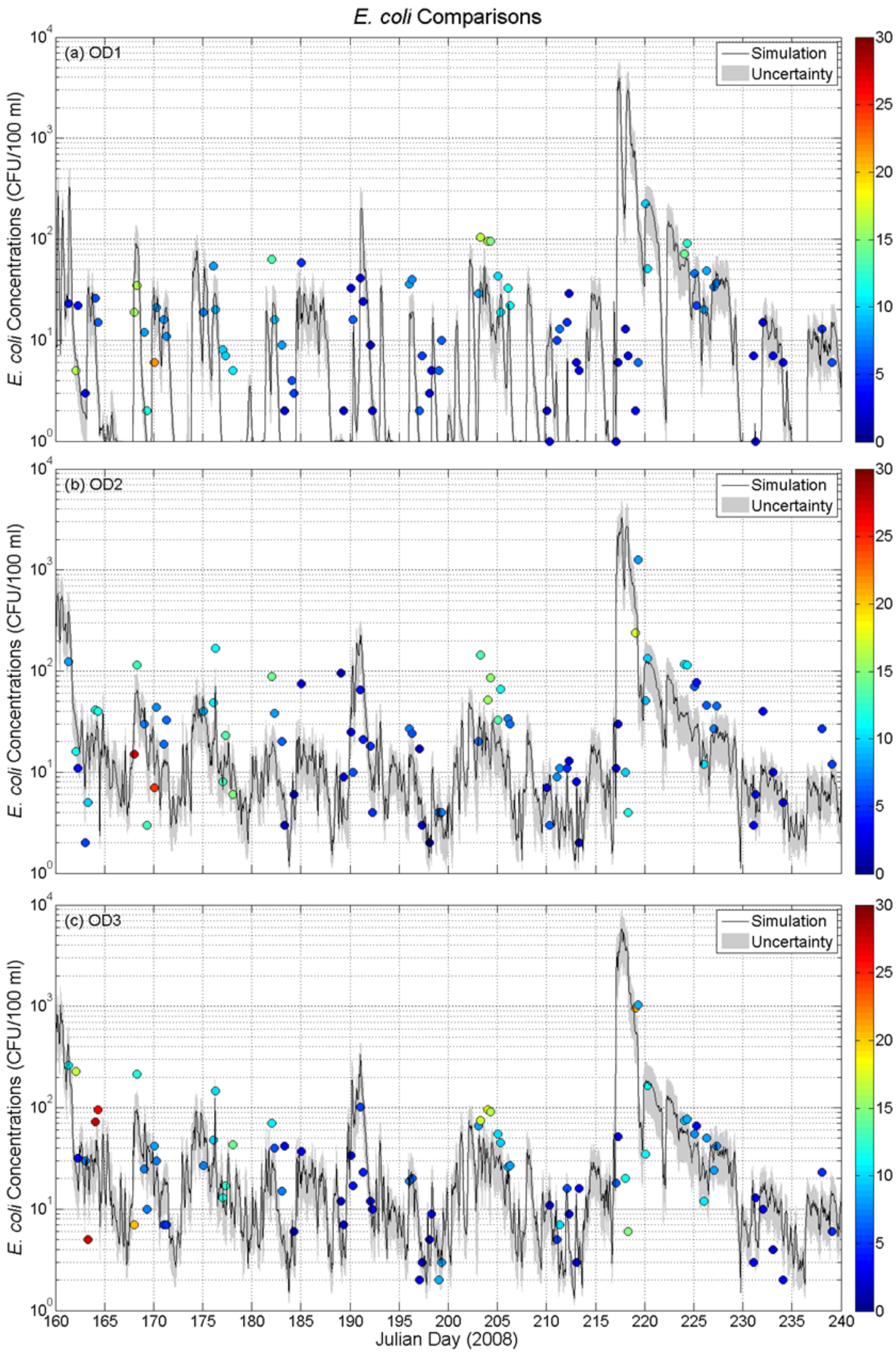

Figure 13: *E. coli* comparison between observed and simulated values with the grey-colored bands representing ± 50% uncertainty in the biological measuremnts at (a) OD1, (b) OD2, and (c) OD3. Turbidity measurements are indicated by the color of each observation point.

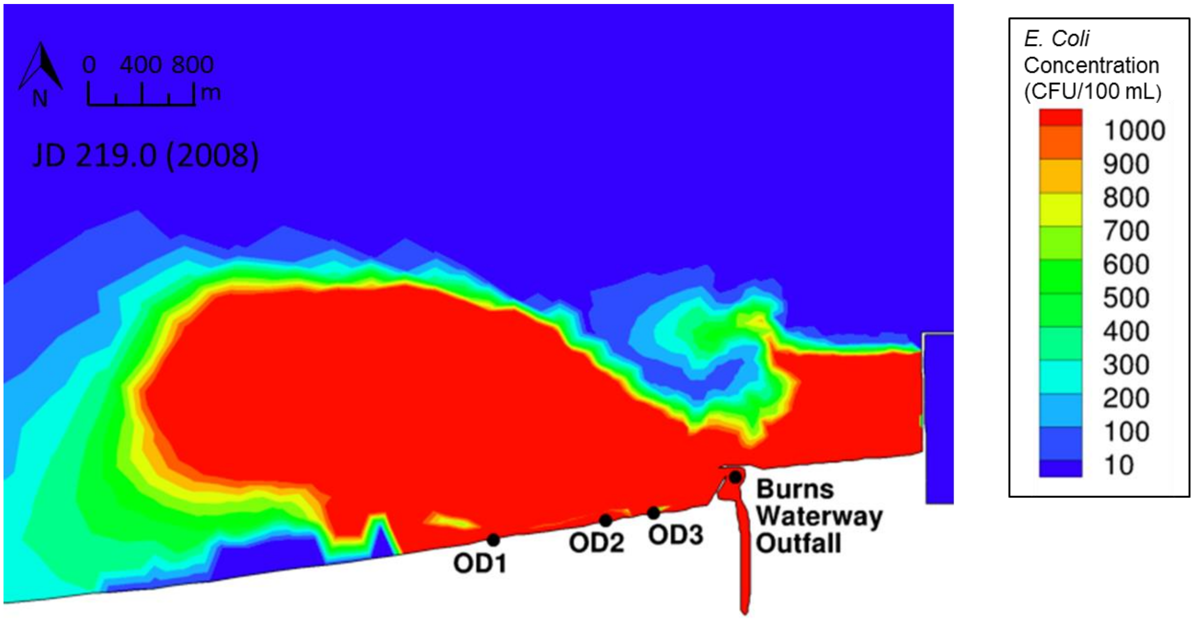

Figure 14: Example of *E. coli* plume in the area of interest

The F_n and the R^2 values of the model (Table 6) for each individual beach indicate that the model does a better job predicting the *E. coli* concentrations at OD2 and OD3 than OD1. The increased distance from the waterway to OD1 (Figure 3) is assumed to be the reason that the model was unable to capture the *E. coli* concentrations in the water. The decreased accuracy at OD1 also aligns with the results of the EC tracer results (Table 3 and Table 4), suggesting that the uncertainty is from the model's ability to describe tracer transport at locations farther from the outfall and not associated with biological processes. The RMSE values (Table 6) for the present model have shown an improvement relative to previous studies reporting RMSE values in the range of 5-10 CFU/100 ml (Connolly et al., 1999) and RMSE values in the range of 1.05-1.36 CFU/100 ml (Thupaki et al., 2013b) for models without sediment transport.

Probability plots of *E. coli* are shown in Figure 15. The comparisons provide further evidence that the model was able to accurately describe the *E. coli* concentrations at the three beach locations; however, the model was better able to describe the concentrations at OD2 and OD3 than OD1, aligning with previous observations.

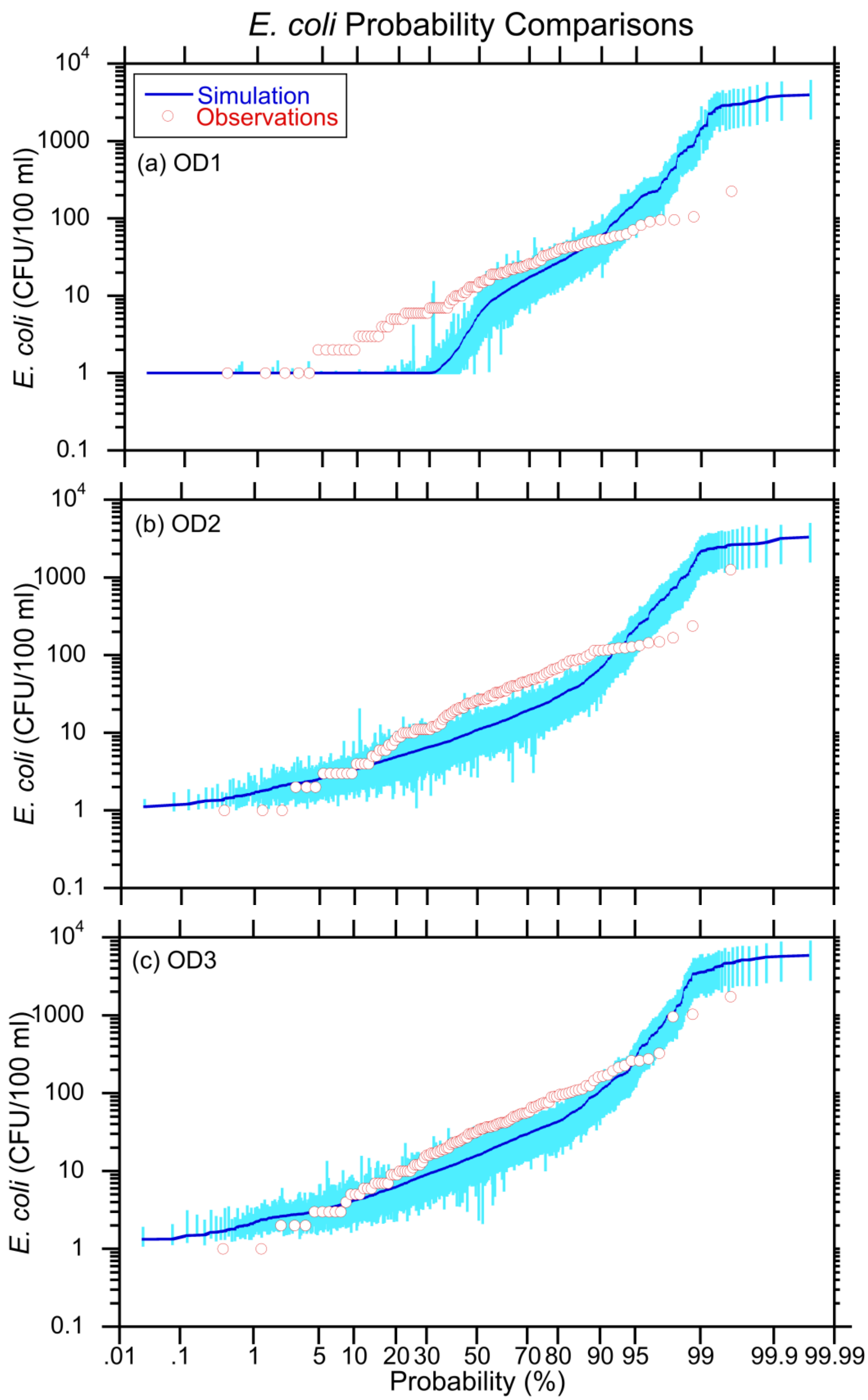

Figure 15: Probability plots for observed values of *E. coli* at OD1, OD2, and OD3 compared with simulated results with the cyan-colored bands representing ± 50% uncertainty in the input from Burns Waterway

The PBIAS of the model indicates that the model had the tendency to over-estimate the *E. coli* concentrations in the water column (Table 6); however, there were still some peaks the model was unable to capture. The upper and lower 50% uncertainty bands for the *E. coli* plots (Figure 13) and the probability plots (Figure 15) shows that the model was unable to explain all of the observational *E. coli* data. The model's inability to describe all the peaks in the FIB data is evidence that either other sources of FIB are present within the area of interest or that *E. coli* life span was inaccurately represented. When *E. coli* is exposed to sunlight, particularly UV bandwidths, it causes the DNA of the *E. coli* to become damaged, inactivating the *E. coli* (Whitman et al., 2004; Sinton et al., 2002), although photo-oxidative effects have been shown to be the main cause of inactivation in surface waters because of the high attenuation of short UV wavelengths (Hipsey et al., 2008). However, the present model does not consider the attenuation characteristics of the different wavelengths within the water column, resulting in an over-estimate of *E. coli* inactivation. This provides one explanation for the model's inability to capture all the peaks. Another cause of decreased simulated *E. coli* concentrations could be due to other *E. coli* sources not incorporated in the model. While it does appear that the major source, Burns Waterway, was identified, other less significant sources of *E. coli* that could affect *E. coli* concentrations in the water column include sediment re-suspension (Thupaki et al., 2013b), anthropogenic activities (Ho et al., 2011), runoff (Jeong et al., 2005), and other point sources (Liu et al., 2006).

3.4 Possible Sources of *E. coli* Concentrations in Burns Ditch

To investigate the other possible sources of FIB concentration near Burns Waterway, the observed *E. coli* data were compared to the flow rate of the waterway recorded from its USGS Gauge (#04095090) location (Figure 16). The comparison shows a correlation between the flow rate of Burns Waterway and the measured *E. coli* values. An increased flow rate is shown between Julian Day 215 and Julian Day 225, indicating that either a large storm event or an increased point source flow rate may have occurred. However, an increased point source flow rate that more than doubles the flow rate of Burns Waterway for a period of 10 days is unlikely; thus it was assumed that the increased flow rate was due to a large precipitation event.

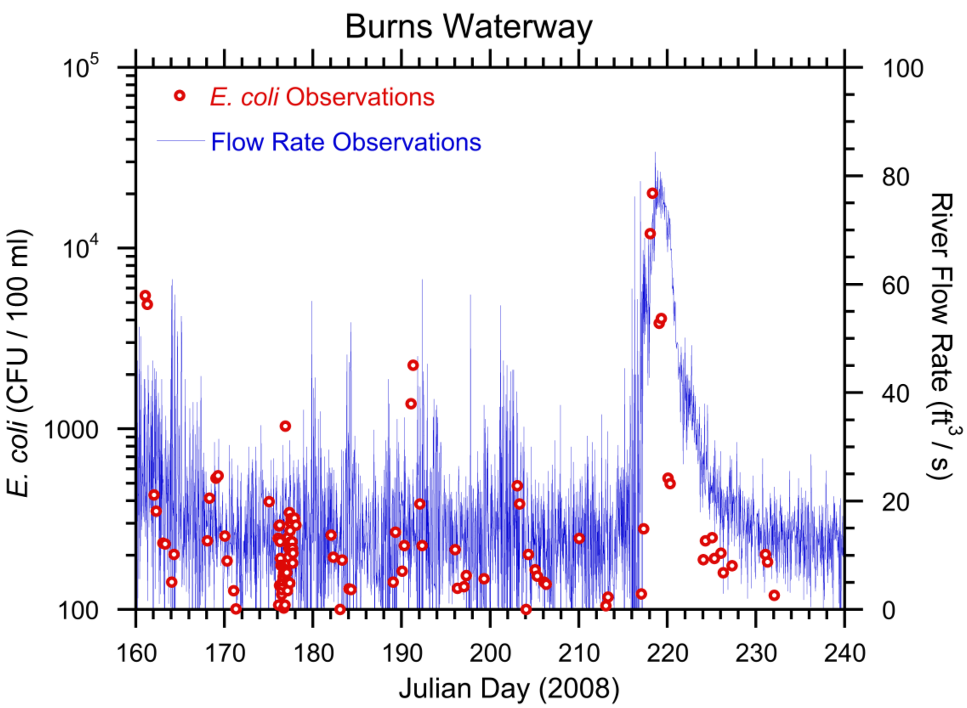

Figure 16: Comparison between Burns Waterway's flow rate and *E. coli* measurements in Burns Waterway

To further investigate the large storm event, observed precipitation data were analyzed from a nearby (~14 km) NCDC Station (#128992) and compared to the *E. coli* measurements in Burns Waterway (Figure 17). The comparison shows a clear relationship between the *E. coli* measurements and the local precipitation. Figures 16 and 17 show that the increased flow rate and the increased *E. coli* measurements are a cause of increased precipitation. While the cause of the increased flow rate is fairly obvious, the relationship between precipitation and increased *E. coli* measurements is not. It is speculated that the increased precipitation led to more run-off in the area, carrying *E. coli* with it into the local waterways, indicating that precipitation data may be a good indicator of *E. coli* concentrations in the water column. This aligns with the work of Jeong et al. (2005), who stated that run-off has a significant impact on the *E. coli* concentrations in the near-shore region.

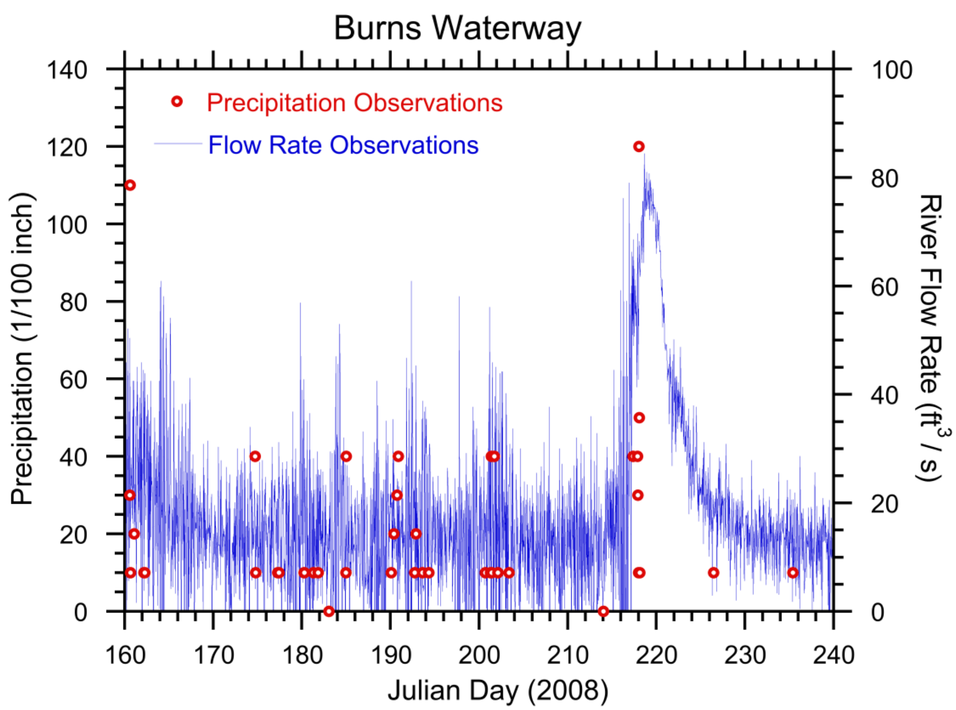

Figure 17: Comparison between Burns Waterway's flow rate and precipitation data measured at NCDC Station #12899

Sediment re-suspension, indicated by turbidity in the water column, was also investigated as a possible source for *E. coli* in the area of interest. Sediments in the near-shore region have been shown to be a significant source of FIB in both marine (Phillips et al., 2011) and freshwater environments (Whitman and Nevers, 2003; Ge et al., 2012a; Thupaki et al., 2013b). Figure 18 shows a comparison between the turbidity and *E. coli* observations at the three sample locations. The comparison shows that the relationship between turbidity and *E. coli* is weak (R^2=0.023), indicating that while turbidity may slightly influence the *E. coli* concentrations in the Ogden Beach region it is not a major source of *E. coli*. Francy and Darner (2002) found a similar relationship between *E. coli* and turbidity with an R^2=0.36. Figure 13 also shows that increased *E. coli* measurements did not occur only when high turbidity was observed.

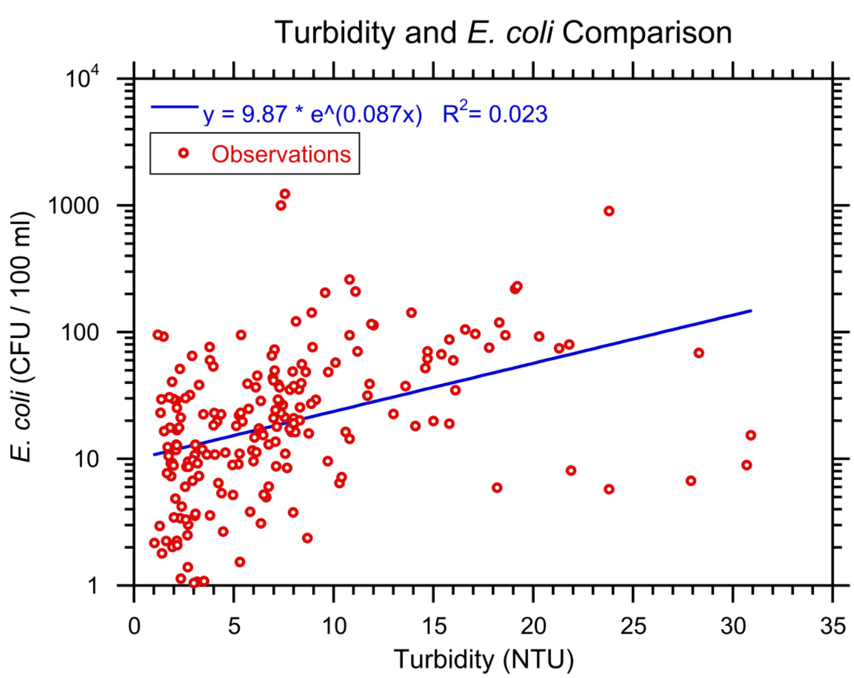

Figure 18: Comparison between turbidity and *E. coli* concentrations in the water column at all three sample locations

3.5 Direct Comparison to a Past Ogden Beach Model

To further compare the present model with the known work of others, the timescale was constrained to that used by Thupaki et al., (2013b), from Julian Day 163 to Julian Day 195 in 2008. Thupaki et al., (2013b) utilized the same observed data as in the present work for their research; however, they applied a structured grid and utilized a sediment transport model to better simulate the interactions between the *E. coli* and suspended sediment. A comparison of a structured grid and unstructured grid model is shown in Figure 19. Since Thupaki et al., (2013b) utilized a structured grid, making it more difficult to resolve the near-shore features, they were unable to resolve all the local features at the Burns Waterway outfall that are important to the transport of *E. coli*, while the present work was able to more accurately resolve the local features using an unstructured grid. A direct comparison between the model grids utilized by Thupaki et al. (2013b) and the present model is shown in Figure 20.

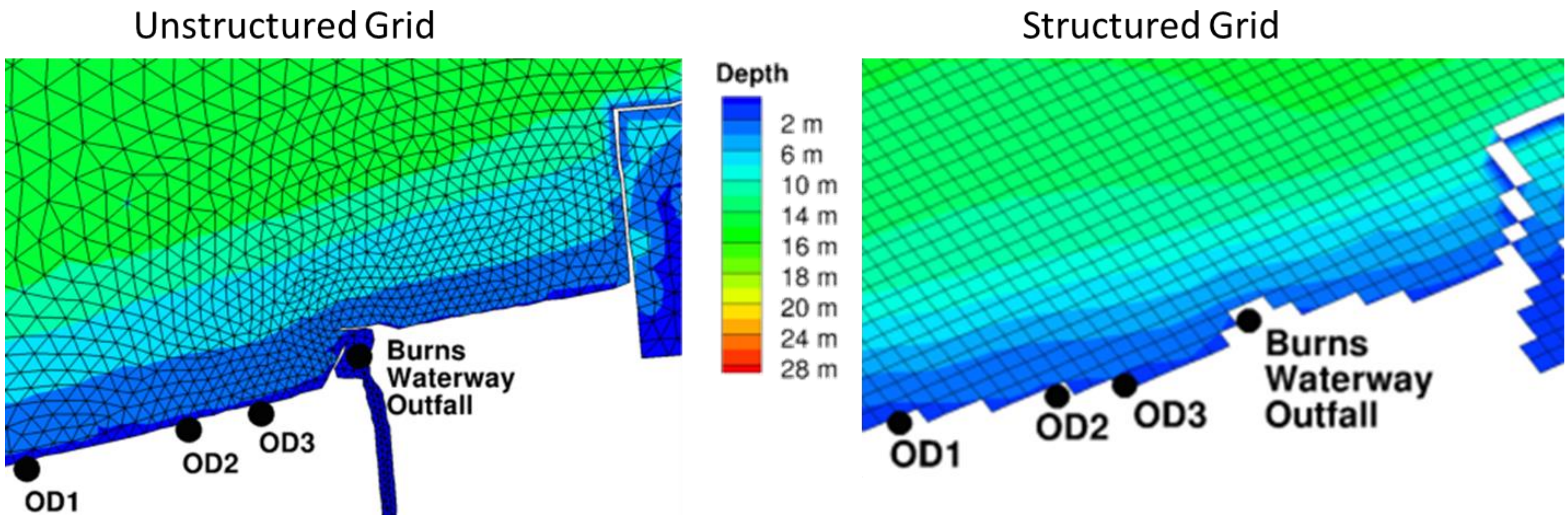

Figure 19: Comparison between an unstructured and structured grid in the area of interest

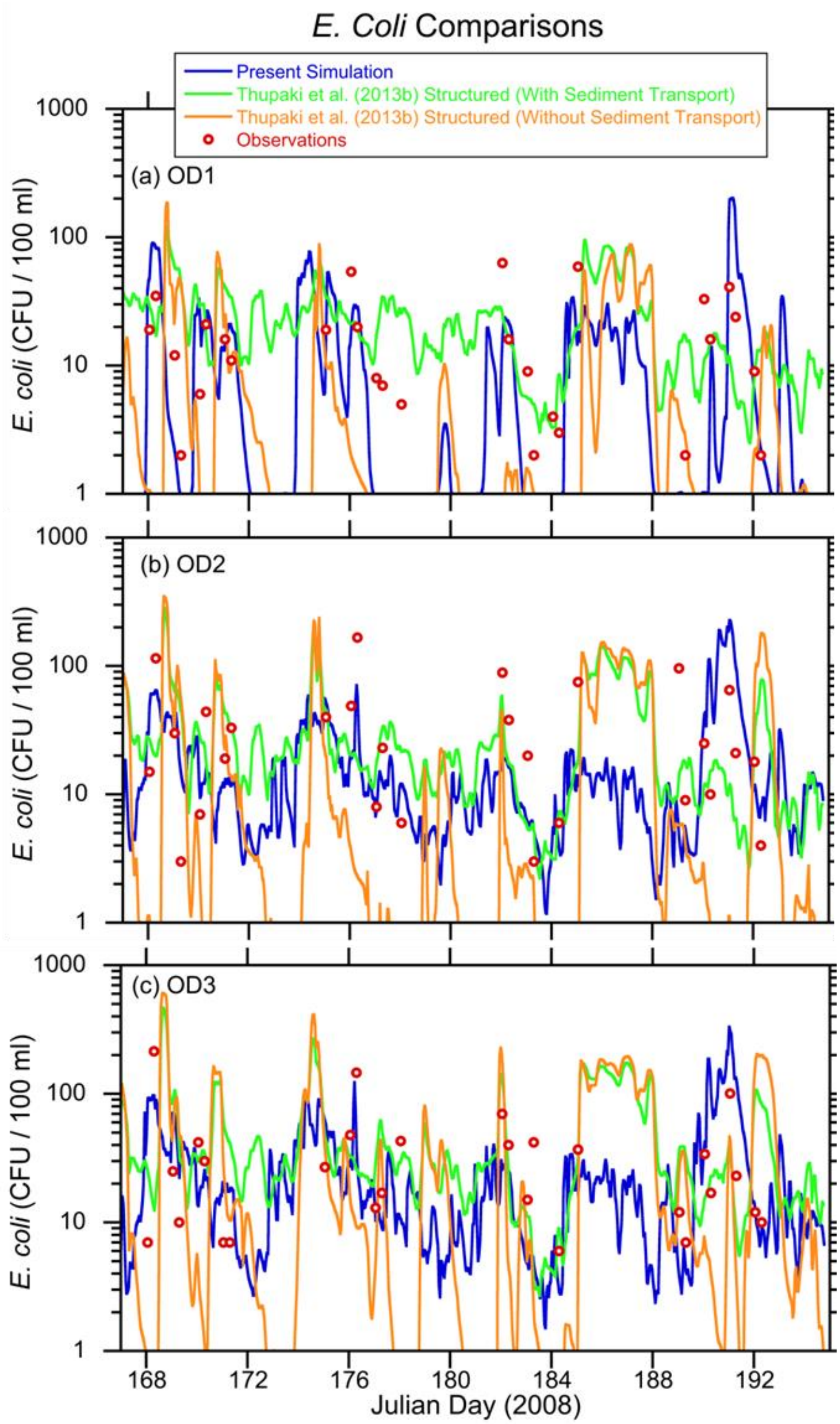

Figure 20: *E. coli* comparison plots between Thupaki et al.'s (2013b) structured grid model and the present unstructured grid model at (a) OD1, (b) OD2, and (c) OD3

Figure 20 indicates that the present model was able to better describe the *E. coli* concentrations at OD1, OD2, and OD3 beach locations than Thupaki et al.'s (2013b) model that did not utilize sediment transport and was comparable to Thupaki et al.'s (2013b) model utilizing sediment transport. Table 7 further verifies this observation from the given RMSE values. The reason for the present model's improvement is thought to be due to the use of an unstructured grid to better represent the near-shore region, particularly the breakwaters influencing the outflow of Burns Waterway, and the ability to constrain the transport model further using the EC concentrations at the beaches.

Table 7: *E. coli* comparison metrics between Thupaki et al.'s (2013b) models (with and without sediment transport) and the present model

	Present Model	**Thupaki et al. (2013b) Structured Grid Models**	
	No Sediment	**No Sediment**	**With Sediment ($K_d = 10\ L\ g^{-1}$)**
Location	**RMSE (CFU/100 ml)**	**RMSE (CFU/100 ml)**	**RMSE (CFU/100 ml)**
OD1	0.75	1.36	0.52
OD2	0.51	1.36	0.53
OD3	0.62	1.05	0.56

Further analysis was performed on the model's ability to predict the median *E. coli* concentrations when compared to Thupaki et al.'s (2013b) models utilizing probability plots (Figure 21). The comparisons further demonstrate the ability of the present model to produce comparable results to Thupaki et al.'s (2013b) structured model utilizing sediment transport and significantly out-perform the simulation not utilizing a sediment transport model, further indicating that an unstructured grid is superior to a structured grid in the near-shore region.

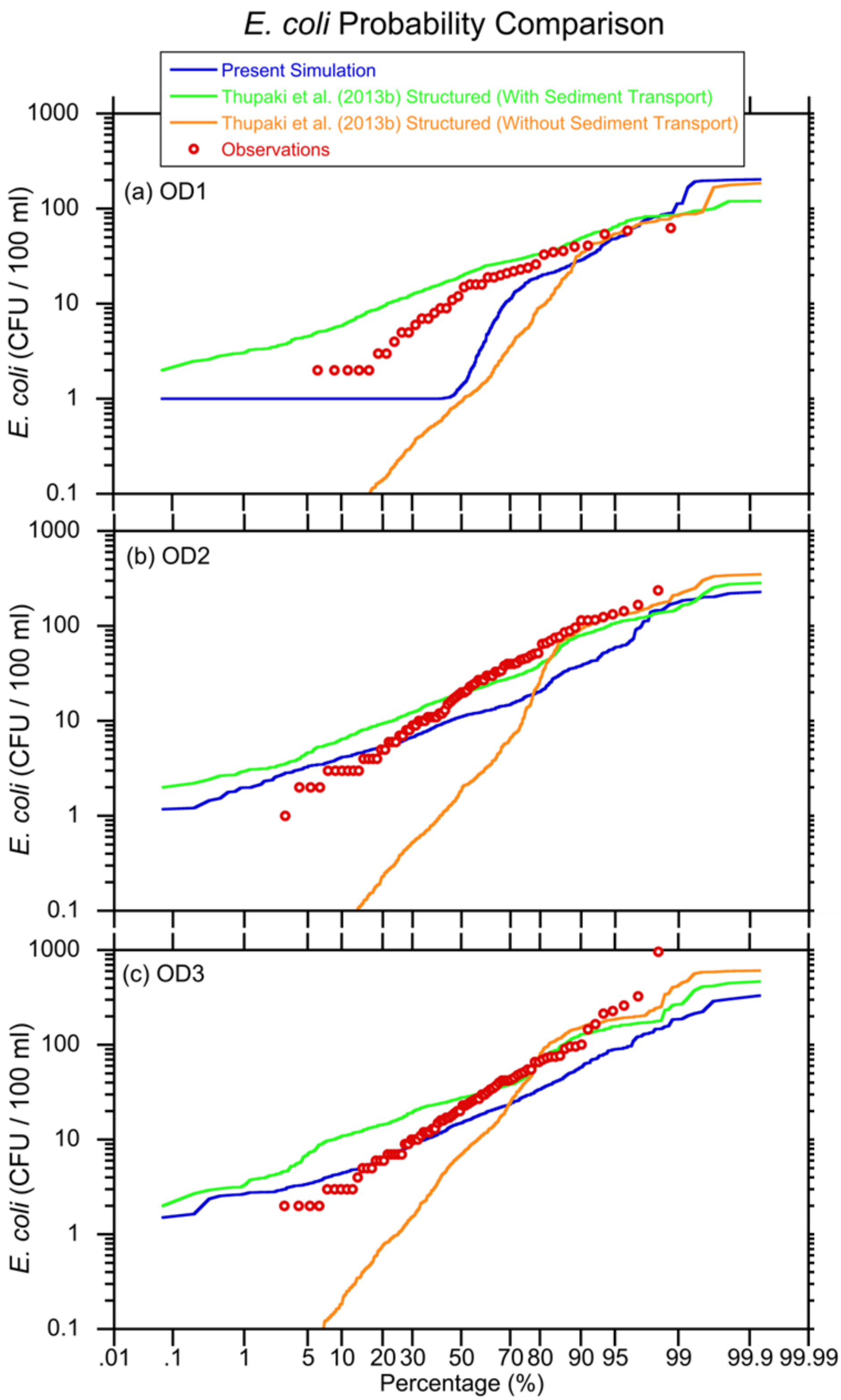

Figure 21: *E. coli* probability plots comparison between Thupaki et al.'s (2013b) structured grid models and the present unstructured grid model at (a) OD1, (b) OD2, and (c) OD3

CHAPTER 4

4.1 Conclusions

A mechanistic model was developed to simulate near-shore contaminant transport utilizing an unstructured, three-dimensional grid. Easily measureable EC values were utilized as a conservative tracer to further constrain the transport model and to verify the near-shore mixing parameters. The transport model was used to predict *E. coli* concentrations at three recreational beaches. After applying a time-varying boundary condition for measured flow and concentrations at the mouth of the river (Burns Waterway's outfall), the following results were found.

4.1.1 Utilizing EC as a Tracer

- Observed EC values were used to constrain the near-shore transport model.

4.1.2 Simulating *E. coli* Concentrations

- The model was able to accurately simulate the *E. coli* concentrations at three beaches in close proximity to Burns Waterway without utilizing a sediment transport model.

4.1.3 Identifying the Source *E. coli* in Burns Waterway

- Utilizing observed *E. coli* concentrations, flow rate measurements, and local precipitation data, run-off was shown to be the primary *E. coli* source within Burns Waterway.

4.1.4 Importance of Unstructured Grids

- The ability to better capture the near-shore features significantly improves the model's ability to predict near-shore contaminants.

Utilizing these results in future models can lead to a more accurate representation of the near-shore water quality parameters, reducing human health risks at local recreational beaches.

BIBLIOGRAPHY

BIBLIOGRAPHY

APHA. Standard Methods for the Examination of Water and Wastewater, 20th ed. (1998)

Surface-water Modeling System. Vers. 11.0.12. Provo: Aquaveo, 2014.

"Testing the Waters 2013 A Guide to Water Quality at Vacation Beaches." *Testing The Waters, Prevent Beach Pollution*. N.p., n.d. Web. 12 Mar. 2014. <http://www.nrdc.org/water/oceans/ttw/in.asp>.

Beletsky, Dmitry, and David J. Schwab. "Modeling Circulation and Thermal Structure in Lake Michigan: Annual Cycle and Interannual Variability." *Journal of Geophysical Research* 106.C9 (2001): 19745-9771. Print.

Connolly, John P., Alan F. Blumberg, and James D. Quadrini. "Modeling Fate of Pathogenic Organisms in Coastal Waters of Oahu, Hawaii." *Journal of Environmental Engineering* 125.5 (1999): 398-406. Print.

Eadie, Brian J. "Probing Particle Processes in Lake Michigan Using Sediment Traps." *Water, Air, & Soil Pollution* 99.1-4 (1997): 133-39. Print.

Eppley, Richard W. "Temperature and Phytoplankton Growth in the Sea." *Fishery Bulletin* 70.4 (1972): 1063-085. Print.

Francy, Donna. S., and Darner, Robert. A., Forecasting Bacteria Levels at Bathing Beaches in Ohio, USGS Fact Sheet FS-132-02 (2002): 4 p

Francy, D. S., E. A. Stelzer, J. W. Duris, A. M. G. Brady, J. H. Harrison, H. E. Johnson, and M. W. Ware. "Predictive Models for Escherichia Coli Concentrations at Inland Lake Beaches and Relationship of Model Variables to Pathogen Detection." *Applied and Environmental Microbiology* 79.5 (2013): 1676-688. Print.

Ge, Zhongfu, Richard L. Whitman, Meredith B. Nevers, and Mantha S. Phanikumar. "Wave-Induced Mass Transport Affects Daily Fluctuations in Nearshore Water." *Environmental Science & Technology* 46.4 (2012): 2204-211. Print.

Ge, Zhongfu Richard L. Whitman, Meredith B. Nevers, Mantha S. Phanikumar and M.N. Byappanahalli. "Nearshore Hydrodynamics as Loading and Forcing Factors for *Escherichia coli* Contamination at an Embayed Beach." *Limnology and Oceanography,* Vol. 57(2012): 362-381. Print

Grunnet, Nicholas M., Dirk-Jan R. Walstra, and B.g. Ruessink. "Process-based Modelling of a Shoreface Nourishment." *Coastal Engineering* 51.7 (2004): 581-607. Print.

Gupta, Hoshin Vijai, Soroosh Sorooshian, and Patrice Ogou Yapo. "Status of Automatic Calibration for Hydrologic Models: Comparison with Multilevel Expert Calibration." *Journal of Hydrologic Engineering* 4.2 (1999): 135-43. Print.

Hipsey, Matthew R., Jason P. Antenucci, and Justin D. Brookes. "A Generic, Process-based Model of Microbial Pollution in Aquatic Systems." *Water Resources Research* 44.7 (2008): 1-26. Print.

Hayashi, Masaki. "Temperature-Electrical Conductivity Relation of Water for Environmental Monitoring and Geophysical Data Inversion." *Environmental Monitoring and Assessment* 96.1-3 (2004): 119-28. Print.

Ho, Lin C., Rachel M. Litton, and Stanley B. Grant. "Anthropogenic Currents and Shoreline Water Quality in Avalon Bay, California." *Environmental Science & Technology* 45.6 (2011): 2079-085. Print.

Jeong, Youngsul, Stanley B. Grant, Scott Ritter, Abhishek Pednekar, Linda Candelaria, and Clinton Winant. "Identifying Pollutant Sources in Tidally Mixed Systems: Case Study of Fecal Indicator Bacteria from Marinas in Newport Bay, Southern California." *Environmental Science & Technology* 39.23 (2005): 9083-093. Print.

Johnson, David, "The Spatial and Temporal Variability of Nearshore Current", PhD Thesis, University of Western Australia (2004). Print.

Legates, David R., and Gregory J. Mccabe. "Evaluating the Use of "goodness-of-fit" Measures in Hydrologic and Hydroclimatic Model Validation." *Water Resources Research* 35.1 (1999): 233-41. Print.

Liu, Lubo, Mantha S. Phanikumar, Stephanie L. Molloy, Richard L. Whitman, Dawn A. Shively, Meredith B. Nevers, David J. Schwab, and Joan B. Rose. "Modeling the Transport and Inactivation of *E. Coli* and Enterococci in the Near-Shore Region of Lake Michigan." *Environmental Science & Technology* 40.16 (2006): 5022-028. Print.

Matlab & Simulink R2012a. Natick: The MathWorks, 2012.

Mclellan, S. L. "Genetic Diversity of Escherichia Coli Isolated from Urban Rivers and Beach Water." *Applied and Environmental Microbiology* 70.8 (2004): 4658-665. Print.

Mellor, George L., and Tetsuji Yamada. "Development of a Turbulence Closure Model for Geophysical Fluid Problems." *Reviews of Geophysics* 20.4 (1982): 851-875. Print.

"Indiana Dunes National Lakeshore (U.S. National Park Service)." *National Parks Service*. U.S. Department of the Interior, 10 Feb. 2014. Web. 12 Mar. 2014. <http://www.nps.gov/indu/index.htm>.

Nearshore Areas of the Great Lakes, 2009. Gatineau, Québec: Environment Canada, 2009. 1-161. Print.

"Nonpoint Source Water Pollution." *IDEM: Water Quality Targets*. N.p., n.d. Web. 12 Mar. 2014. <http://www.in.gov/idem/nps/3484.htm>.

Environmental Protection Agency Water Quality Office. Effect of geographical location on cooling pond requirement and performance. Technical report, Environmental Protection Agency, March 1971.

Parkinson, Claire L., and Warren M. Washington. "A Large-Scale Numerical Model of Sea Ice." *Journal of Geophysical Research* 84.C1 (1979): 311. Print.

Phillips, Matthew C., Helena M. Solo-Gabriele, Alan M. Piggot, James S. Klaus, and Yifan Zhang. "Relationships between Sand and Water Quality at Recreational Beaches." *Water Research* 45.20 (2011): 6763-769. Print.

Schimmelpfennig, Sebastian, Georgiy Kirillin, Christof Engelhardt, and Gunnar Nützmann. "Effects of Wind-driven Circulation on River Intrusion in Lake Tegel: Modeling Study with Projection on Transport of Pollutants." *Environmental Fluid Mechanics* 12.4 (2012): 321-39. Print.

Sinton, L. W., C. H. Hall, P. A. Lynch, and R. J. Davies-Colley. "Sunlight Inactivation of Fecal Indicator Bacteria and Bacteriophages from Waste Stabilization Pond Effluent in Fresh and Saline Waters." *Applied and Environmental Microbiology* 68.3 (2002): 1122-131. Print.

Smagorinsky, J. "General Circulation Experiments With The Primitive Equations." *Monthly Weather Review* 91.3 (1963): 99-164. Print.

R. D. I. Teledyne. Self-Contained ADCP Applications: WinSC and PlanADCP User's Guide. Teledyne, R. D. I., 2006.

Thupaki, Pramod, Mantha S. Phanikumar, Kmitry Beletsky, David J. Schwab, Meredith B. Nevers, and Richard L. Whitman. "Budget Analysis of Escherichia Coli at a Southern Lake Michigan Beach." *Environmental Science & Technology* 44.3 (2010): 1010-016. Print.

Thupaki, Pramod, Mantha S. Phanikumar, and Richard L. Whitman. "Solute Dispersion in the Coastal Boundary Layer of Southern Lake Michigan." *Journal of Geophysical Research: Oceans* 118.3 (2013): 1606-617. Print.

Thupaki, Pramod, Mantha S. Phanikumar, David J. Schwab, Meredith B. Nevers, and Richard L. Whitman. "Evaluating the Role of Sediment-bacteria Interactions Onconcentrations at Beaches in Southern Lake Michigan." *Journal of Geophysical Research: Oceans* 118.12 (2013): 7049-065. Print.

Walstra, D.J.R., Sutherland, J., Hall, L., Blogg, H., Ormondt, M.v., 2001. Verification and comparison of two hydrodynamic area models for an inlet system. In: Hanson, H., Larson, M. (Eds.), Proc. 4th Int. Conf. on Coastal Dynamics ’01. ASCE, Reston, Virginia, pp. 433-42.

Whitman, R. L., and M. B. Nevers. "Foreshore Sand as a Source of Escherichia Coli in Nearshore Water of a Lake Michigan Beach." *Applied and Environmental Microbiology* 69.9 (2003): 5555-562. Print.

Whitman, R. L., M. B. Nevers, G. C. Korinek, and M. N. Byappanahalli. "Solar and Temporal Effects on Escherichia Coli Concentration at a Lake Michigan Swimming Beach." *Applied and Environmental Microbiology* 70.7 (2004): 4276-285. Print.